NPS -57Li72011A

NAVAL POSTGRADUATE SCHOOL

Monterey, California

STUDIES PERTAINING TO SOLID PROPELLANT FRACTURE

by

Gerald Gilbert

G. H. Lindsey

31 January 1972

This document has been approved for public release and sale; its distribution is unlimited.

FEDDOCS
D 208.14/2:NPS-57Li72011A

TL785
.L73

LIBRARY
NAVAL POSTGRADUATE SCHOOL
MONTEREY, CALIF. 93940

NAVAL POSTGRADUATE SCHOOL
Monterey, California

Rear Admiral A. S. Goodfellow, Jr.
Superintendent

M. U. Clauser
Academic Dean

ABSTRACT:

This study of propellant fracture has been subdivided into three parts: (1) pertinent elastic fracture developments, (2) viscoelastic fracture, and (3) dewetting.

In (1) a fracture criterion is developed for stress fields producing mixed mode crack propagation by drawing a comparison with fracture in uncracked geometries. Such mixed fields are prevalent for cracks in rocket motors with star shaped cavities.

In (2) a means for predicting crack growth and velocity has been developed for linear viscoelastic meterials strictly on the basis of stress intensity factors. A fracture characterization of critical stress intensity factor for a CTPB propellant has been completed, which facilitates the application of the theory.

In (3) extensive dewetting experiments have been completed which have confirmed prior theoretical developments of a quasielastic dewetting theory. Not only has the concept of a stress criterion for dewetting been substantiated, but the form of the surface predicted by the theory has been verified.

FOREWORD

This report summarizes the results of work on a research project entitled Propellant Fracture Studies, which is funded by the Naval Weapons Center, China Lake, California.

The report is prepared in three sections. The first section contains ideas and observations concerning elastic fracture in combined symmetric and skew symmetric stress fields. Validation of the theory is made with glassy polymers, and the work was performed as a precursor to formulating similar results for viscoelastic materials.

Section 2 deals directly with viscoelastic crack propagation in symmetric modes and develops a much more simplified theory than exists in the literature for handling viscoelastic fracture . The author would like to acknowledge many discussions of this material with LCDR C. Hertzler.

Section 3 deals with dewetting, which is the phenomenon that makes propellant different from ordinary viscoelastic materials. Extensive studies of dewetting have been reported previously on this contract and this section continues the report of those studies. Acknowledgement is given to LCDR J. E Wood, who has contributed some of the results of his PhD thesis work, which is on this topic, for this report.

TABLE OF CONTENTS

Page

SECTION 1 SOME OBSERVATIONS ON ELASTIC FRACTURE UNDER COMBINED LOADING. 1

Introduction. 1

Correlation of Fracture Criteria. 3

Example Plexiglass. 6

Subsequent Behavior 12

Summary 16

SECTION 2 VISCOELASTIC FRACTURE 17

Introduction. 17

Stress Analysis 18

Fracture Postulate. 22

Fracture Characterization 24

Data Reduction. 29

Solution Method 34

Conclusions 35

SECTION 3 DEWETTING 36

Introduction. 36

Dilatometer Tests 37

Constant Load Dilatometer Tests 37

Constant Strain Rate Dilatometer Tests. 39

Pokerchip Triaxial Tension Test 41

Results 43

Comparison of Experimental Data with Theoretical Criterion 49

SECTION 4 CONCLUSION. 52
REFERENCES 54
APPENDIX A EXTENDED CORRESPONDENCE PRINCIPLE 56
Definition of the Problem 56
Extension of Graham's Paper 61
APPENDIX B STRESS ANALYSIS OF AN INFINITE STRIP. 63
Elastic Stress Analysis of Strip. 63
Displacement Boundary Conditions. 66
DISTRIBUTION LIST. 69
FORM DD 1473 70

English Symbols

a^e, b^e, c^e = elastic boundary quantities

a^v, b^v, c^v = viscoelastic boundary quantities

b = strip width

B, B_1, B_2 = definition of boundary

c = crack length

E = modulus

f, g, F, G, Φ = general functions

G = shear modulus

h = heaviside step function

I_1, I_2, J_2 = stress invariants

K = bulk modulus

K_1, K_2 = stress intensity factor

r = polar coordinates

t_1 = time of arrival of crack

t = sheet thickness or time

U_i = displacement

u = strain energy

x, y = cartesian coordinates

Greek Symbols

α = experimental constant

β = crack orientation angle

ϵ_{ij} = strain

λ = Geometric factor

ν = Poissons ratio

Φ = stress function

σ_{ij} = stress

$\sigma, \sigma_n, \sigma_s$ = applied stress at the boundary

θ = polar coordinate

SECTION 1

SOME OBSERVATIONS ON ELASTIC FRACTURE UNDER COMBINED LOADING

INTRODUCTION

Much of the traditional theory of fracture has been cast in terms of failure surfaces in principal stress space, which have been given physically descriptive names such as maximum principal stress, distortional energy, etc, and these theories have been applied to bodies that are assumed to contain no dominant flaws. On the other hand, in more recent times an equally strong theory in the form of "fracture mechanics" has been developed upon the premise that a crack already exists within the body. As a result of these two developments, fracture analysis is compartmentalized into problems of one type or the other.

The two approaches have been further dissimiliar in the types of stress fields typically treated. While the use of combined stress states is very common in the instance of failure surface theories, it is not at all common to apply fracture mechanics to combined loading conditions, and in fact a general criterion is not available where more than one mode of fracture is present. In this report an attempt is made to bridge between the two for elastic materials, linking them more closely together and providing a more unified perspective. By bringing both of these theories together, a general fracture criterion has emerged for combined loading and mixed mode crack propagation.

Work on the problem of crack propagation in sheets under combined loads was undertaken by Erdogan and Sih[1], who proposed an explanation of crack trajectories in plane two dimensional stress fields based upon experimental results obtained with PMM (polymethylmethacrylate). Later Panasyuk, et al[2] independently proposed similar explanations based upon their work with glass. Cottrell[3], has examined the energy released from a system when a crack extends radially along an arbitrary trajectory. He found that the direction of propagation hypothesized by the above investigators corresponds to the direction of maximum energy release, which is consistent with the general fracture theory proposed by Griffith.

In the experimental studies that were conducted relative to the before mentioned investigations, the stress conditions which precipitated crack instability were only of secondary interest; consequently observations are offered herein to complete the picture by describing the local conditions of fracture at a crack tip in an arbitrary two dimensional stress field by relating them to fracture conditions in unflawed geometries. This leads quite naturally to a fracture criterion representable in K_1-K_2 space. From this development further observations can be made regarding the changing nature of the stress field in the vicinity of a crack as it continues to propagate under combined loading. Verification of the theory has been demonstrated on PMM for two dimensional plane geometries.

Interest in the combined loading fracture conditions arises for solid propellant rocket grains since many of the cracks in rocket motors are subjected to both symmetric and anti symmetric loads.

CORRELATION OF FRACTURE CRITERIA

For the unflawed case, i.e., for specimens without cracks, fracture in multiaxial stress states is describable in terms of a surface in principal stress space. Over the years, it has been found by experience that the continuous surfaces are quadric surfaces and are representable by second order equations in stress. A very general representation of such surfaces can be made in terms of the first two stress invariants I_1 and I_2; however it is physically more meaningful to use I_1 and J_2, the second deviatoric stress invariant. The equation of the surface in functional form is

$$f\ (I_1^2,\ J_2) = 0 \tag{1.1}$$

where I_1^2 is selected for dimensional homogeniety.

Mathematical expressions such as equation (1.1) represent the manner in which a material reacts fracturewise to applied loads and theoretically will predict fracture regardless of the geometry or character of the stress state. A crack in a body introduces a geometrical change, but it should not influence the fundamental fracture behavior. Therefore a similar function should exist, which is related to this one, and which describes fracture of cracked bodies.

For geometries containing cracks, Barenblatt[4] has proposed that the local distribution of cohesive forces over the crack surface at fracture is a material property, independent of external loading and body geometry; thus for any body constructed of a given material there exists a function of stress intensity factors which describes elastic fracture conditions. For two dimensional stress states limited to the opening and sliding mode, his criterion reduces to

$$\Phi\,(-K_{1a},\ -K_{2a}) = 0 \tag{1.2}$$

where K_{1a} and K_{2a} are the portion of the stress intensity factors which are due to the cohesive forces at the crack tip. The total stress intensity factor is obtained by adding the cohesive force contribution to K_1 and K_2, which result from the external forces.

$$K_{1t} = K_1 + K_{1a} \qquad K_{2t} = K_2 + K_{2a} \tag{1.3}$$

By Barenblatt's[5] hypothesis of no singularity at the crack tip

$$K_1 = -K_{1a} \qquad K_2 = -K_{2a} \tag{1.4}$$

Thus from equations (1.2) and (1.4)

$$\Phi\,(K_1,\ K_2) = 0 \tag{1.5}$$

To relate f in equation (1.1) to Φ in equation (1.5), $\Phi(K_1,\ K_2)$ will be expressed in terms of invariants. The stress field in the vicinity of a crack, when cohesive forces are not considered, may be written as

$$r^{\frac{1}{2}}\ \sigma_{ij} = K_1\ F_{ij}\ (\theta) + K_2\ G_{ij}\ (\theta) \qquad i,j = 1,2 \tag{1.6}$$

From this equation, one can solve for K_1 and K_2 in terms of the two in-plane principle stresses or in terms of the two stress invariants, both of which can be used to relate fracture of cracked geometries to fracture of uncracked geometries. Continuing in terms of invariants, equation (1.6) can be used to formulate $I_1^{\,2}$ and J_2.

$$r\ I_1^2 = f_1 (K_1, K_2, \theta) \tag{1.7a}$$

$$r\ J_2 = f_2 (K_1, K_2, \theta) \tag{1.7b}$$

Solving for K_1 and K_2 and inserting them into (1.5) produces a description of the local conditions governing fracture at a pre-existant crack

$$\Phi\ (rJ_2, rI_1^2) = 0 \tag{1.8}$$

This describes the conditions of crack propagation in some direction, θ_0, of the maximum tensile stress, as referenced from the original crack orientation. It disregards the cohesive forces and expresses the fracture condition in terms of the externally applied loads only, just as the fracture surface does. On the other hand, the success of the fracture surface concept over a wide variety of stress states and body shapes makes evident the fact that the fracture behavior of an elastic material is independent of the geometry of the body of interest, and it will not be altered in a fundamental way by the introduction of different geometric factors, such as cracks. It seems, therefore, appropriate to offer as a hypothesis that, when only external forces are considered, "Fracture will occur in cracked geometries at the same local stress conditions which produce fracture in uncracked geometries." In other words, the crack will extend when the invariants of stress on the trajectory satisfy equation (1.1) and equation (1.8). This can be expressed mathematically as

$$\Phi = f \tag{1.9}$$

In other words, if the fracture surface f is known, the fracture condition, Φ, for bodies containing cracks may be obtained by replacing J_2 and I_1^2 with r J_2 and rI_1^2. From this a general fracture criterion can be generated in terms of K_1 and K_2.

EXAMPLE PLEXIGLASS

Figure 1-1 shows the uncracked multiaxial fracture behavior of PMM obtained by Thorkildsen and Olszewski[6], where it has been plotted in two dimensional principal stress space. A more precise reduction of this data in terms of invariants makes possible the correlation with results obtained by Erdogan and Sih[1] on cracked specimens made from the same material.

Stress invariants, I_1 and I_2, are defined as:

$$I_1 = \sigma_1 + \sigma_2 + \sigma_3 \tag{1.10a}$$

$$I_2 = -(\sigma_1 \sigma_2 + \sigma_2 \sigma_3 + \sigma_1 \sigma_3) \tag{1.10b}$$

A plot was made in Figure 1-2 of I_2 vs I_1^2 for the experimental data, which appears to yield a clearly defined linear relationship. The data was fitted by least squares to a linear equation, which resulted in

$$-I_1^2 = -2.93I_2 + 0.96\sigma_u^2 \tag{1.11}$$

where σ_u is the failure stress in uniaxial tension. This expression in terms of invariants is postulated to be the description of a failure surface for all possible tensile stress states. Instead

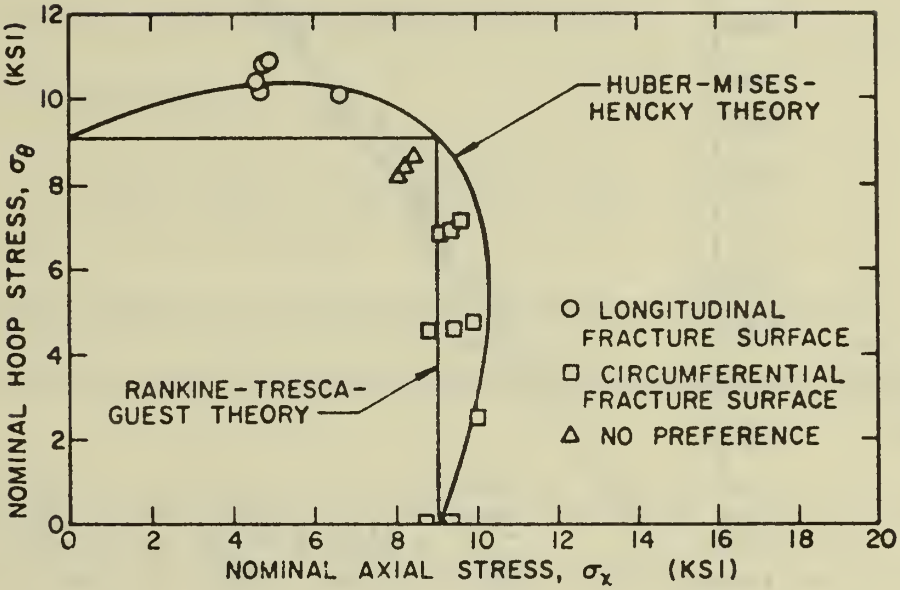

FIG. 1-1 FRACTURE STRESS FOR POLY (methylmethacrylate) (Thorkildsen and Olszewski[6])

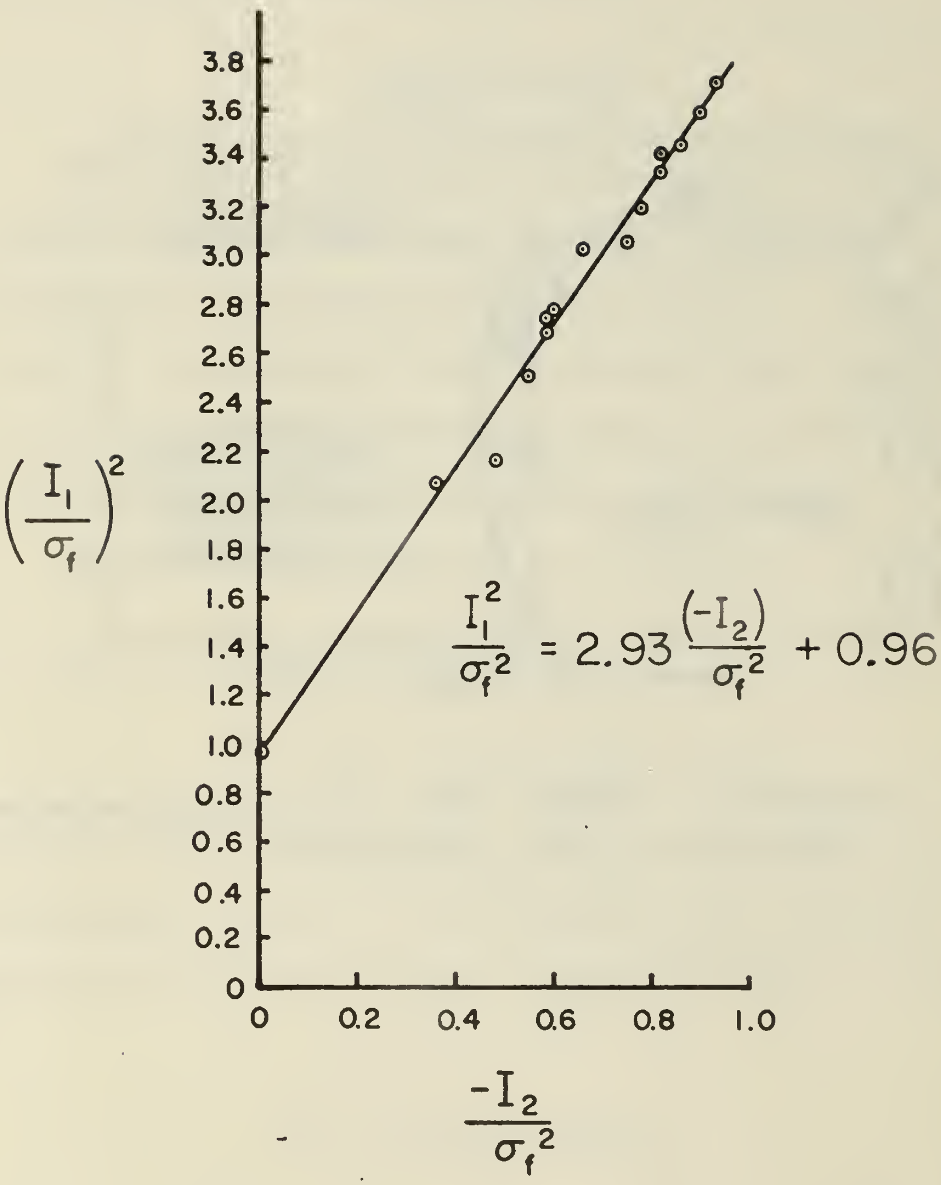

FIG. I-2 LEAST SQUARES FIT TO FRACTURE DATA FOR PMM

of leaving the final expression in terms of I_2, which has no particular physical interpretation, it is preferred to use J_2, which is related to I_1 and I_2 by

$$J_2 = \frac{I_1^2}{3} + I_2 \tag{1.12}$$

Using (1.11) and (1.12) an expression for the failure surface of PMM is found to be of the form,

$$f(I_1^2, J_2) = J_2 + 0.007 I_1^2 - \text{Const} = 0 \tag{1.13}$$

As can be seen, there is a very slight dependency on hydrostatic pressure, but shear is the predominant factor for fracture in tension of PMM.

As stated previously, it is proposed that this criterion also governs the onset of crack propagation for bodies containing residual cracks in the same type of material. In other words, for bodies containing a crack, fracture will occur by an incremental extension of the crack along the path normal to the greatest tension when the stresses on that trajectory combine to satisfy the fracture criterion found for uncracked specimens. This requires that the direction of propagation, θ_0, be known a priori; however this information can be calculated from the work of Erdogan and Sih. By equations (1.8), (1.9) and (1.13), propagation of a crack is given by

$$rJ_2 + .007\, rI_1^2 - \text{Const} = 0 \tag{1.14}$$

To apply this criterion, the crack tip stress field is used. The coordinate description is standard, and the equations are classical as given by Sih and Liebowitz[7].

$$\sigma_r = \frac{1}{2(2r)^{\frac{1}{2}}} \text{Cos } \frac{\theta}{2} \left[(3 - \text{Cos } \theta)K_1 + (3 \text{ Cos } \theta - 1)K_2 \text{ Tan } \frac{\theta}{2}\right] \qquad (1.15a)$$

$$\sigma_\theta = \frac{1}{2(2r)^{\frac{1}{2}}} \text{Cos } \frac{\theta}{2} \left[(1 + \text{Cos } \theta)K_1 - 3K_2 \text{ Sin } \theta\right] \qquad (1.15b)$$

$$\tau_{r\theta} = \frac{1}{2(2r)^{\frac{1}{2}}} \text{Cos } \frac{\theta}{2} \left[K_1 \text{Sin}\theta + K_2(3 \text{ Cos } \theta - 1)\right] \qquad (1.15c)$$

J_2 in polar coordinates is given by,

$$J_2 = \frac{1}{3}\left[\sigma_r^2 - \sigma_r\sigma_\theta + \sigma_\theta^2 + 3\tau_{r\theta}^2\right] \qquad (1.16)$$

which in terms of stress intensity factors from equations (1.15) give

$$rJ_2 = \frac{1}{6} \left\{\frac{1}{8}\left[7 + 4 \text{ Cos}\theta - 3 \text{ Cos } 2\theta\right] K_1^2 + \left[3/2 \text{ Sin } 2\theta - \text{Sin } \theta\right]K_1K_2 + \frac{1}{2}\left[7 - \text{Cos } \theta - \frac{9}{2} \text{Sin}^2 \theta\right]K_2^2\right\} \qquad (1.17)$$

From equations (1.15), I_1^2 can also be readily computed,

$$r\, I_1^2 = 2\left[K_1^2 \text{ Cos}^2 \frac{\theta}{2} - K_1K_2 \text{ Sin}\theta + K_2^2\text{Sin}^2 \frac{\theta}{2}\right] \qquad (1.18)$$

Combining equations (1.17) and (1.18) for a surface of the general form that was exhibited by PMM in equation (1.14), we have

$$r(J_2 + \alpha I_1^2) = \frac{1}{6}\left\{\left[\frac{1}{8}(7+4 \text{ Cos}\theta - 3 \text{ Cos } 2\theta) + 6\alpha(1 + \text{Cos } \theta)\right] K_1^2 + \left[\left(\frac{3}{2} \text{ Sin } 2\theta - \text{Sin}\theta\right) - 12\,\alpha \text{ Sin}\theta\right] K_1K_2 + \left[\frac{1}{2}\left(7 - \text{Cos}\theta - \frac{9}{2}\text{Sin}^2\theta\right) + 6\alpha(1 - \text{Cos}\theta)\right] K_2^2\right\} \qquad (1.19)$$

The constant in (1.14) is found by examining the fracture condition of symmetric loading, for which $K_1 \rightarrow K_{1C}$, $K_2 = 0$ and $\theta_o = 0$. From (1.19)

$$[r(J_2 + \alpha I_1^2)] = \text{Const} = \frac{1}{6}(1+12\alpha)\, K_{1C}^{\;2} \tag{1.20}$$

Thus the criterion of fracture for arbitrary combined loads is given by

$$\begin{aligned}(1 + 12\alpha)K_{1C}^2 &= \left[(\tfrac{7}{8} + 6\alpha) + (\tfrac{1}{2} + 6\alpha)\operatorname{Cos}\theta - \tfrac{3}{8}\operatorname{Cos} 2\theta\right] K_1^2 \\ &\quad + \left[\tfrac{3}{2}\operatorname{Sin} 2\theta - (1+12\alpha)\operatorname{Sin}\theta\right] K_1K_2 \\ &\quad + \left[(\tfrac{7}{2} + 6\alpha) - (\tfrac{1}{2} + 6\alpha)\operatorname{Cos}\theta - \tfrac{9}{4}\operatorname{Sin}^2\theta\right] K_2^2\end{aligned} \tag{1.21}$$

where for PMM, $\alpha = 0.007$.

To limit check the skew-symmetric fracture condition, $K_1 = 0$, $K_2 \rightarrow K_{2C}$ and Erdogan and Sih's theory and measurements give $\theta_o = -70.5°$. Equation (1.21) gives the critical K_2 value in terms of the critical K_1 value,

$$K_{2C} = \left[\frac{3\,(1 + 12\alpha)}{4\,(1 + 3\alpha)}\right]^{\frac{1}{2}} K_{1C} \tag{1.22}$$

Substantiation of this prediction from the theory is provided by the experimental results of Erdogan and Sih, who found for PMM, $K_{1C} = 472$ lb in$^{-3/2}$ and $K_{2C} = 422.1$ lb in$^{-3/2}$. Using this value of K_{IC} in (1.22), and $\alpha = .007$ from (1.14) the theory predicts $K_{2C} = 421.5$ lb in$^{-3/2}$. This very close correlation provides meaningful substantiation to the theory.

Further evaluation of the theory can be obtained by plotting equation (1.21) for a variety of combined loading conditions. For any given angle of propagation, θ_o, the fracture equation (1.21) is an inclined ellipse in K_1, K_2 space. However in K_1, K_2 space, each set of coordinates dictates a different loading condition, which requires the angle of propagation to be different, and the coefficients in the fracture equation vary, deviating from an ellipse. A plot of the equation is given in figure 1-3, where it is compared with the data of Erdogan and Sih for a variety of combined loading conditions obtained by using the geometry of a crack inclined to the direction of applied loads for several different crack orientation angles, β. As can be seen, the theory fits the data quite well for strongly skew-symmetric loadings, but deviates somewhat in some of the loadings that are predominantly symmetric. Of course for those loadings that are purely symmetric, the criterion matches identically due to the fact that the governing equation was matched to this condition.

SUBSEQUENT BEHAVIOR

After the crack has begun to run under combined loads, the geometry will appear as depicted in figure 1-4 for small extensions. A solution of this problem has been obtained by Andersson[8], wherein he found that the stress intensity factors K_1 and K_2 are

$$\hat{K}_1 = \sigma \sqrt{c} \left[\frac{\pi - \theta_o}{\pi + \theta_o}\right]^{\frac{\theta_o}{2}} \text{Sin } \beta \text{ Sin } (\beta + \theta_o)$$

$$\hat{K}_2 = \sigma \sqrt{c} \left[\frac{\pi - \theta_o}{\pi + \theta_o}\right]^{\frac{\theta_o}{2}} \text{Sin } \beta \text{ Cos } (\beta + \theta_o) \qquad (1.23)$$

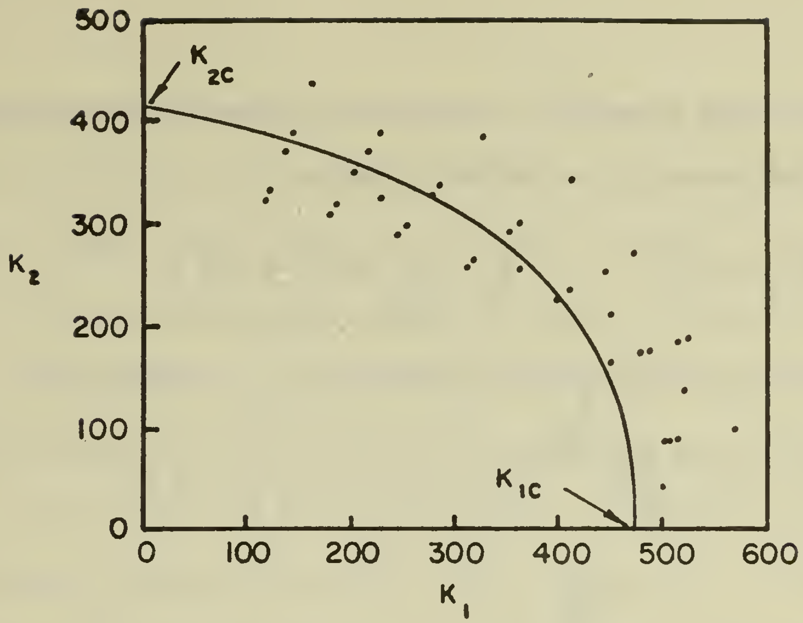

FIG. 1-3 K_1 VERSUS K_2 AT THE BEGINNING OF CRACK EXTENSION IN A CRACKED PLATE UNDER PLANE LOADING.

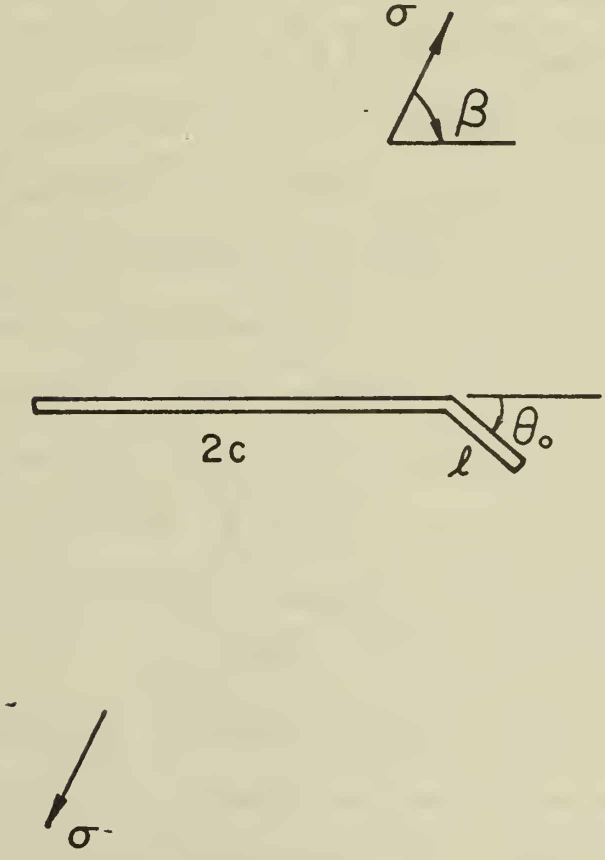

FIG. 1-4 GEOMETRY OF CRACK AFTER EXTENSION UNDER COMBINED LOADS.

However before the crack extended, the stress intensity factors were those of an inclined crack in an infinite sheet.

$$K_1 = \sigma\sqrt{c}\ \mathrm{Sin}^2\beta \qquad K_2 = \sigma\sqrt{c}\ \mathrm{Sin}\ \beta\ \mathrm{Cos}\ \beta \tag{1.24}$$

When these expressions are substituted into (1.23) it reduces to

$$\begin{aligned} \hat{K}_1 &= \left[\frac{\pi - \theta_o}{\pi + \theta_o}\right]^{\frac{\theta_o}{2}} [K_1\ \mathrm{Cos}\ \theta_o - K_2\ \mathrm{Sin}\ \theta_o] \\ \hat{K}_2 &= \left[\frac{\pi - \theta_o}{\pi + \theta_o}\right]^{\frac{\theta_o}{2}} [-K_1\ \mathrm{Sin}\ \theta_o - K_2\ \mathrm{Cos}\ \theta_o] \end{aligned} \tag{1.25}$$

This set of equations suggests that, in effect, propagation can be considered as a rotation of the K_1K_2 axis system, and from the experimental evidence available, the rotation is such that it reduces the value of K_2. In other words the crack, operating under the observed laws of behavior mentioned previously, will propagate in the direction of the maximum tension and this will reduce the value of K_2. Furthermore by extrapolation, subsequent increments of propagation will be along the direction of instantaneous maximum tension, which will continue to reduce K_2, driving it to zero so that ultimately propagation continues in the direction normal to the maximum tensile field stress of the body.

To illustrate this, consider figure 1-4 as an example, where $\ell = 0$ and $\beta = 70^\circ$. The angle of maximum tension is $\theta_o = -30^\circ$, or $-\pi/6$. The corresponding point on the fracture envelope in K_1, K_2 space from (1.21) and (1.24) is $K_1 = 442$ lb in$^{-3/2}$ and $K_2 = 155$ lb in$^{-3/2}$. After propagating an infinitesimal amount, ℓ, the new stress intensity factors from (1.25) are $K_1 - 447.4$ lb $\text{in}^{-3/2}$ and $K_2 = 84.3$ lb $\text{in}^{-3/2}$. Thus in the first infinitesimal increment of propagation, K_2 is reduced by 46%. This change in K_2, which produces a change in the loading that the crack sees, causes a change in the stress field. These changes reduce K_2 further, and this interaction continues until K_2 is nonexistent and the crack is propagating in a symmetrically loaded condition.

Another interesting way of looking at equation (1.25) is to take) the square root of the sum of squares. This results in

$$[\hat{K}_1^2 + \hat{K}_2^2]^{\frac{1}{2}} = f(\theta_o)[K_1^2 + K_2^2]^{\frac{1}{2}} \tag{1.26}$$

In K_1, K_2 space the square root of the sum of squares is the length of a position vector. Since $f(\theta_o) \leq 1$, this equation shows that the position vector to the fracture envelope in K space is becoming shorter, or that the "resultant" stress intensity factor is growing smaller as the crack propagates. If it decreases by a sufficient amount, the crack should stop. The maximum reduction for the first increment occurs at the largest θ_o, which is produced by pure shear loading. In that instance $\theta_o = -70.5^\circ$, for which $f(\theta_o) = 0.85$. This turns out to be enough to stop propagation of the crack after it has begun. In the experimental results of Erdogan and Sih on PMM in pure shear, the crack subjected to pure shear stopped after propagating a short distance; however, this was the only crack geometry studied for which the crack stopped close to where it had begun to propagate.

These observations have been discussed within the context of experimental data on PMM and glass. Similar data on inclined cracks in plates are not available for metals. If they were, the validity of the observations could be checked further and the influence of plastic yielding could also be studied; however preparation of metallic sheet specimens with real cracks of arbitrary angles of inclination is quite difficult. Meanwhile the available evidence on two elastic materials appears to substantiate a correlation between the two failure domains.

SUMMARY

Observations have been made which link fracture criteria in unflawed specimens to crack instability in bodies containing residual cracks, and from this a criterion for fracture under arbitrary loading is postulated in terms of an envelope in stress intensity factor space. Furthermore an explanation is offered for crack behavior subsequent to the onset of propagation which is based upon the concepts generated concerning the surface in stress intensity factor space. Experimental results for two materials, glass and polymethylmethoerylate, verify the theory for two dimensional, combined loadings involving the opening mode and the sliding mode of crack propagation.

SECTION 2

VISCOELASTIC FRACTURE

SECTION 2

VISCOELASTIC FRACTURE

Introduction

In the last three years viscoelastic fracture theory has been advanced along much more fruitful avenues than those which the previous efforts produced. By applying principles of conservation of energy at the crack tip, Knauss[10] has shown that a differential equation governing crack length history can be generated. Several of his works continue this development, and in each case an unknown length parameter manifests itself in the differential equation. The parameter, which must be determined experimentally, seems to be inherent to the method of solution.

Since this parameter is a bother to deal with and since it is artificial in the sense that there is no physical basis for its existence, it was felt that a worthwhile contribution could be made by devising a means of formulating viscoelastic fracture without the parameter. The means by which this was finally done was through the viscoelastic correspondence principle.

The classical correspondence principle normally applied in the solution of boundary value problems in the linear, quasi-static theory of viscoelastic, does not apply for crack propagation problems. In that instance new boundary is being created as the crack propagates, and the conditions on the boundary are changing in type; i.e. they are changing from displacement to stress boundary conditions and vice versa. In this kind of problem there will be points of the boundary where only partial histories of the boundary conditions are known; consequently the integral Laplace Transform cannot be computed, and the correspondence principle is not applicable.

Graham [9] has extended the correspondence principle to encompass problems of this type. (An explanation of his development is given in Appendix A.) By using Graham's method of solution, two very large categories of problems have been solved. Linking these solutions with Knauss' experimental findings and theoretical concepts has lead to a method of viscoelastic fracture analysis based upon stress intensity factors. The method parallels elastic fracture theory very closely and combines the work of other investigators in such a way that the length parameter is no longer needed.

Stress Analysis

One very common class of crack problems for which the extended correspondence principle is applicable is shown in Figure 2-1, where the lower portion of the body has been removed and replaced with appropriate boundary conditions. The two solutions by Graham[27] in the literature that use the extended correspondence principle are for bodies of infinite extent. However the method is applicable to finite geometries. In the case of stress boundary conditions, like those pictured in Figure 2-1, the application is quite simple. In the case of displacement boundary conditions, which is treated later, the boundary conditions have to be recast into an acceptable form; therefore

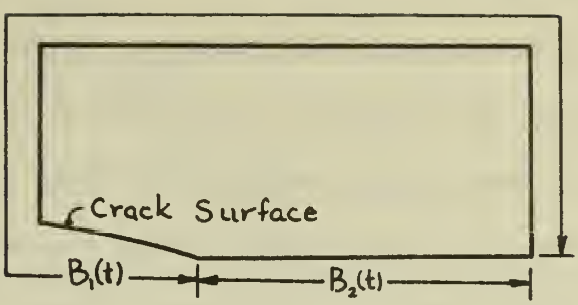

Figure 2-1 Definition of boundaries for the Correspondence Principle

the boundaries may be finite or infinite. They are loaded with normal stresses and are free of shear stress. The stress distributions are symmetric so that displacements on the imaginary extension in front of the crack are zero. The boundary conditions vary with time according to the following description:

$$\begin{aligned} \sigma_s &= 0 && \text{on } B \\ \sigma_n &= B(x,t) && \text{on } B_1(t) \\ u_n &= 0 && \text{on } B_2(t) \end{aligned} \tag{2.1}$$

These conditions correspond to column 2 of the matrix given in equation (A.1) of Appendix A.

The extension of the correspondence principle by Graham permits the construction of the viscoelastic solution for a moving crack from an elastic solution for a moving crack. This in turn may be generated from the stresses and displacements of a stationary crack. For an incompressible elastic body, the field quantities in the neighborhood of the crack tip are given by

$$\sigma_{ij} = \frac{K_1}{\sqrt{2\pi r}} f_{ij}(\theta) \tag{2.2a}$$

$$u_i = \frac{3K_1}{8E}\sqrt{\frac{2r}{\pi}}\, g_i(\theta) \tag{2.2b}$$

The crack is now imagined to propagate slowly. For most elastomers and all propellants, the velocity of propagation is quite low, which makes the inertial terms in the equations of motion small and neglectable. Therefore the stress and displacement fields are the same as those given in equation (2) except that the coordinate system to which the above quantities are referenced is now moving since it is attached to the crack tip. The dynamic, elastic solution is

$$\sigma^e_{ij}(t) = \frac{K^e_1(t)}{\sqrt{2\pi r(t)}}\, f_{ij}[\theta(t)] \tag{2.3a}$$

$$u^e_i(t) = \frac{3}{8}\,\frac{K^e_1(t)}{E}\sqrt{\frac{2r(t)}{\pi}}\, g_i[\theta(t)] \tag{2.3b}$$

It is a simple matter to reference these quantities to an inertial coordinate system. As stated previously the loading and geometry is taken such that only the opening mode of propagation is present; therefore

$$r(t)\cos\theta(t)+c(t) = x \tag{2.4}$$

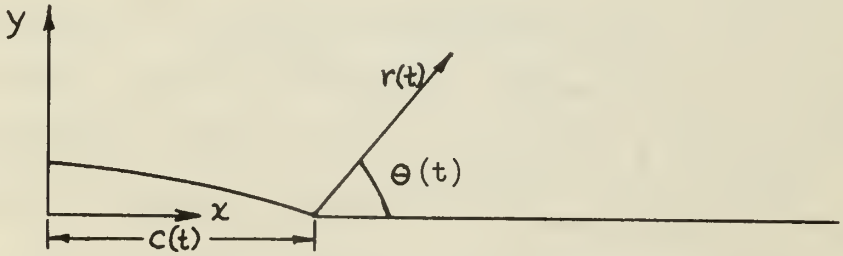

Figure 2-2 Inertial Coordinate System

Equations (2.3) for the dynamic elastic problem became

$$\sigma^{e}_{ij}(t) = \frac{K^{e}_{1}(t)}{\sqrt{2\pi(x-c(t))}} F_{ij}[\theta(t)] \tag{2.4a}$$

$$u^{e}_{i}(t) = \frac{3}{8}\,\frac{K^{e}_{1}(t)}{E}\sqrt{\frac{2(x-c(t))}{\pi}}\; G_{i}[\theta(t)] \tag{2.4b}$$

To use the correspondence principle, the transform of equation (2.4) is needed.

$$\sigma^{e*}_{ij} = \left[\frac{K^{e}_{1}(t)}{\sqrt{2\pi[x-c(t)]}} \quad F_{ij}[\theta(t)]\right]^{*} \tag{2.5a}$$

$$u^{e*}_{i} = \frac{3}{8E}\left[K^{e}_{1}(t)\sqrt{\frac{2[x-c(t)]}{\pi}} \quad G_{i}[\theta(t)]\right]^{*} \tag{2.5b}$$

By equations (A.4) of Appendix A,

$$\sigma^{v*}_{ij} = \left[\frac{K^{e}_{1}(t)}{\sqrt{2\pi[x-c(t)]}} \qquad F_{ij}[\theta(t)]\right]^{*}_{\substack{E\rightarrow E*\\ \nu\rightarrow\nu*}} \tag{2.6a}$$

$$u^{e*}_{i} = \frac{3}{3E*}\left[K^{e}_{1}(t)\sqrt{\frac{2[x-c(t)]}{\pi}} \qquad G_{i}[\theta(t)]\right]^{*}_{\substack{E\rightarrow E*\\ \nu\rightarrow\nu*}} \tag{2.6b}$$

For elastic stress intensity factors in which there are no material properties, equation (2.6a) is readily inverted and yields

$$\sigma^{v}_{ij}(t) = \sigma^{e}_{ij}\ (t) \tag{2.7}$$

From this result, by comparison of the terms,

$$K^{v}_{1}(t) \equiv K^{e}_{1}(t) \tag{2.8}$$

where the stress intensity factor for viscoelastic materials is defined to be the same as for the elastic case. Indeed when the boundary conditions are all in terms of stress, the two are identical, which indicates that the definition chosen is consistent. In other words, we are here defining the viscoelastic stress intensity factor as that factor which when multiplied by $\frac{F_{ij}[\theta(t)]}{\sqrt{2\pi(x-c(t))}}$ gives the stress components in the vicinity of the crack tip. This definition possesses the appropriate form as one proceeds to the limit of elastic materials. Also the stress intensity factor, contains information concerning geometry and boundary conditions, as it does in the case of elastic materials.

For many geometries fitting the boundary conditions of equation (2.1), the elastic stress intensity factor is

$$K_1 = \lambda\sigma\sqrt{\pi c} \tag{2.9}$$

where λ is a geometric modifiying factor that can be independent of time, but is often a function of c. If σ is the applied stress at the boundary, then

$$K_1^v(t) = K_1^e(t) = \lambda[c(t)]\sigma(t)\sqrt{\pi c(t)} \tag{2.10}$$

Fracture Postulate

Fracture studies in recent years have led to the conclusion that flaws in materials will grow when under load. This continues until the flaw becomes of critical size, at which time the specimen undergoes unstable crack propagation and fracture. This has been found to be true for metals, especially in fatigue, and for nonmetals alike.

Knauss[10] has published theoretical developments of these ideas for viscoelastic materials and has shown that the important parameter of interest for rate sensitive materials is crack velocity. In the elastic case, the threshold of rapid crack propagation is often the focus of interest; however in viscoelastic materials the crack is found to propagate for almost any load level. The velocities are infinitesimally small for low loads and increase as the body is more highly stressed. The question to be answered then becomes, not at what load level does the crack propagate but what is the crack velocity for any given load. As defined, the viscoelastic stress intensity factor contains information relative to the boundary conditions; therefore we desire the relationship between stress intensity factor and crack velocity.

This brings us to the fracture postulate:

If $[K_1^V(t)]_{\text{Body 1}} = [K_1^V(t)]_{\text{Body 2}}$

then $[\dot{c}(t)]_{\text{Body 1}} = [\dot{c}(t)]_{\text{Body 2}}$

In words this states that for every stress intensity factor there is a corresponding unique crack velocity.

Knauss[11] has performed experiments on Solithane 113, a polyurethane elastomer, which have substantiated this to a degree (Francis et al [12] have duplicated these tests and done additional work on other types of loads.) For all temperature ranges tested, the material was elastic in the sense that it did not relax; however the crack behavior was viscoelastic and exhibited a velocity that varied with loading. Knauss postulates that in this type of material when the strain at the crack tip is the same in two different bodies, the same crack velocity will be produced. Of course in a body that is behaving elastically so far as stress and strain are concerned, the same strain level is equivalent to the same stress intensity factor. Thus in the postulate of fracture, we are following the previous ideas of Knauss. Furthermore, it states that if the stress intensity factor history can be calculated, the crack velocity equation can be determined from the experimental characterization of the material. Once this is known, the crack history can be obtained by quadrature. This will be demonstrated later.

Fracture Characterization

Fracture characterization has been done for only a few materials, and it has normally been accomplished with an infinite strip containing a semi-infinite crack. It could just as well have been done, however, on the sheet with the internal crack that was described earlier in this section.

To apply the correspondence principle, we appeal to the extended version in Appendix A. The geometry is shown in Figure 2-3, where the boundary is given a normal displacement in the vertical direction on B_3.

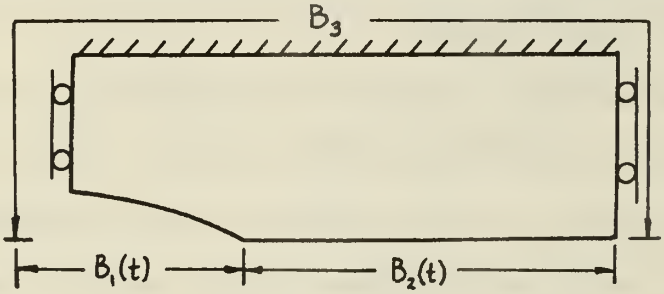

Figure 2-3 Displacement Boundary Conditions

The actual boundary conditions are given below.

$$\begin{aligned} \sigma_s^v &= 0 && \text{on } B_1(t) \\ \sigma_n^v &= 0 && \text{on } B_1(t) \\ u_n^v &= 0 && \text{on } B_2(t) \\ u_s^v &= 0 && \text{on } B_2(t) \\ u_n^v &= U_n(x,t) && \text{on } B_3 \\ u_s^v &= U_s(x,t) && \text{on } B_3 \end{aligned} \tag{2.11}$$

These must be redefined in terms that will satisfy the conditions of the extended correspondence principle. This can be accomplished with the following set:

$$\begin{aligned}
u_n^v &= A^v(x,t) && \text{on } B_1(t) + B_2(t) \\
\sigma_s^v &= 0 && \text{on } B_1(t) \\
u_s^v &= 0 && \text{on } B_2(t) \\
u_n^v &= U_n(x,t) && \text{on } B_3 \\
u_s^v &= U_s(x,t) && \text{on } B_3
\end{aligned}$$

The normal displacements are specifiable over the crack surface without material properties because the far field boundary conditions are on displacements. This now allows the construction of an equivalent elastic problem, whose boundary conditions are

$$\begin{aligned}
u_n^e &= A^e(x,t) && \text{on } B_1(t) + B_2(t) \\
\sigma_s^e &= 0 && \text{on } B_1(t) + B_2(t) \\
u_n^e &= U_n(x,t) && \text{on } B_3 \\
u_s^e &= U_s(x,t) && \text{on } B_3
\end{aligned}$$

Since the transforms are known for all time,

$$\begin{aligned}
u_n^{e*} &= A^{e*}(x,p) && \text{on } B_1(t) + B_2(t) \\
\sigma_s^{e*} &= 0 && \text{on } B_1(t) + B_2(t) \\
u_n^{e*} &= U_n^{*}(x,p) && \text{on } B_3 \\
u_s^{e*} &= U_s^{*}(x,p) && \text{on } B_3
\end{aligned}$$

represent the boundary conditions to the corresponding viscoelastic problem. From Graham the viscoelastic solution is obtained from (A.4).

The stress intensity factors for the strip are developed in Appendix B. Using the results of equation (B.20a) in equation (2.5) for $\nu = \frac{1}{2}$,

$$\sigma_{ij}^{e*} = \sqrt{\frac{4b}{3}}\, E \left[\frac{\varepsilon_o(t)}{\sqrt{2\pi[x-c(t)]}} \right]^* F_{ij}(0) \qquad \theta = 0 \tag{2.12a}$$

$$u_i^{e*} = \frac{\sqrt{3b}}{2} \left[\varepsilon_o(t) \sqrt{\frac{2[x-c(t)]}{\pi}}\, G_i(\pi)\, \delta \right]^* \quad \begin{array}{l} x < c_o,\ \delta = 1 \\ x > c_o,\ \delta = h(t-t_1) \end{array} \tag{2.12b}$$

By the correspondence principle

$$\sigma_{ij}^{v*} = \sqrt{\frac{4b}{3}}\, E_{REL}^{*}\, p \left[\frac{\varepsilon_o(t)}{\sqrt{2\pi[x-c(t)]}} \right]^* F_{ij}(0) \tag{2.13a}$$

$$u_i^{v*} = \frac{\sqrt{3b}}{2} \left[\varepsilon_o(t) \sqrt{\frac{2[x-c(t)]}{\pi}}\, G_i(\pi)\, \delta \right]^* \tag{2.13a}$$

Inverting the transforms, the viscoelastic solution is obtained.

$$\sigma_{ij}^{v}(t) = \sqrt{\frac{4b}{3}} \left\{ \frac{E_{REL}(t)\varepsilon_o(0^+)}{\sqrt{2\pi(x-c_o)}} + \int_0^t E_{REL}(t-\tau) \frac{d}{d\tau} \left[\frac{\varepsilon_o(\tau)}{\sqrt{2\pi[x-c(\tau)]}} \right] d\tau \right\} F_{ij}(0) \tag{2.14a}$$

$$u_i^{v}(t) = \frac{\sqrt{3b}}{2}\, \varepsilon_o(t) \sqrt{\frac{2[x-c(t)]}{\pi}}\, G_i(\pi)\, \delta \tag{2.14b}$$

It is evident from these equations that now the simpler expressions are the displacements, since the boundary conditions are of that type. The stresses are now more complex due to the material properties that are contained in the stress intensity factor.

For a step strain history, which is most usually the one that is applied,

$$\varepsilon_o(t) = e_o 1(t) \tag{2.15}$$

The stresses and displacements reduce to

$$\sigma^{v}_{ij}(t) = \sqrt{\frac{4b}{3}} \left\{ \frac{2E_{REL}(t)e_{o}}{\sqrt{2\pi(x-c_{o})}} + \pi e_{o} \int_{o}^{t} \frac{E_{REL}(t-\tau)\dot{c}(\tau)}{[2\pi[x-c(\tau)]]^{3/2}} d\tau \right\} F_{ij}(0) \tag{2.16a}$$

$$u^{v}_{i}(t) = \frac{\sqrt{3b}}{2} e_{o} \sqrt{\frac{2[x-c(t)]}{\pi}} G_{i}(\pi)\delta \tag{2.16b}$$

The stress intensity factor, by comparison with equation (2.4a), and by the previously given definition would be

$$K^{v}_{1}(t) = \sqrt{\frac{8\pi b}{3}[x-c(t)]} e_{o} \left\{ \frac{2E_{REL}(t-\tau)}{\sqrt{2\pi[x-c_{o}]}} + \pi \int_{o}^{t} \frac{E_{REL}(t-\tau)\dot{c}(\tau)}{[2\pi[x-c(\tau)]]^{3/2}} d\tau \right\} \tag{2.17}$$

This is a very complicated expression, and one not very conducive to data reduction from laboratory results. However, a very good approximation can be made, which makes the data reduction quite simple.

A distance out in front of the crack in the strip, the stress field is that of a strip without a crack. If the specimen is long enough compared to the crack, a large portion of the body will be subject to the stress given in equation (B.17). With that approximation, the stress intensity factor is

$$K^{e}_{1}(t) = \sqrt{\frac{3b}{4}} \sigma(t) \tag{2.18}$$

where $\sigma(t)$ is the stress acting on the strip computed on the basis of the net cross-sectional area, i.e. with the crack length removed. In that case, from equation (2.5a)

$$\sigma^{e*}_{ij} = \sqrt{\frac{3b}{4}} \left[\frac{\sigma(t)}{\sqrt{2\pi[x-c(t)]}} \right]^{*} F_{ij}(0) \tag{2.19}$$

Because there are now no material properties in the expression $\sigma_{ij}^{v*} = \sigma_{ij}^{e*}$ and

$$\sigma_{ij}^{v}(t) = \sqrt{\frac{3b}{4}} \; \frac{\sigma(t)}{\sqrt{2\pi[x-c(t)]}} \; F_{ij}(0) \tag{2.20}$$

Therefore the viscoelastic stress intensity factor is

$$K_1^{v}(t) = \sqrt{\frac{3b}{4}} \; \sigma(t) \tag{2.21}$$

Since the displacements are fixed at the boundary, the stresses in the strip are relaxing, and $K_1^{v}(t)$ will be decreasing in time as the crack propagates. This can be shown from the viscoelastic stress-strain relationships obtainable from the elastic solution of Appendix B. Equation (B.17) for an incompressible material gives

$$\sigma = \sqrt{\frac{4}{3}} \, E \, \epsilon_o \tag{2.22}$$

By the regular correspondence principle, the stress in the viscoelastic strip is expressed in the classical form.

$$\sigma(t) = \frac{4}{3} \int_{0^-}^{t} E_{REL}(t-\tau) \, \frac{d\epsilon_o(\tau)}{d\tau} \, d\tau \tag{2.23}$$

For a step strain history, equation (2.15),

$$\sigma(t) = \frac{4}{3} \, e_o \, E_{REL}(t) \tag{2.24}$$

and the viscoelastic stress intensity factor of equation (2.21) can be expressed in an alternate form

$$K_1^{v}(t) = \sqrt{\frac{4}{3}b} \; e_o \, E_{REL}(t) \tag{2.25}$$

Either equation (2.25) or (2.21) can be used for data reduction.

Data Reduction

For each different level of e_o there will be a different crack velocity history produced. Unfortunately it is not constant in time because the stress in equation (2.21) is not constant. Parenthetically it should be stated here that if a means for experimentally applying a constant stress boundary condition could be employed, then the results of the first case of Appendix B could be used and nothing would vary with time in the strip. For a given level of stress the stress intensity factor would remain constant, since it is independent of crack length; consequently the crack velocity would be constant, and it would be a very desirable test. In fact it would be just like the elastic case for which this test has been used by Knauss for a number of years

Returning to data reduction, the stress and crack length in the strip are recorded as a function of time, as shown in Figure 2-4.

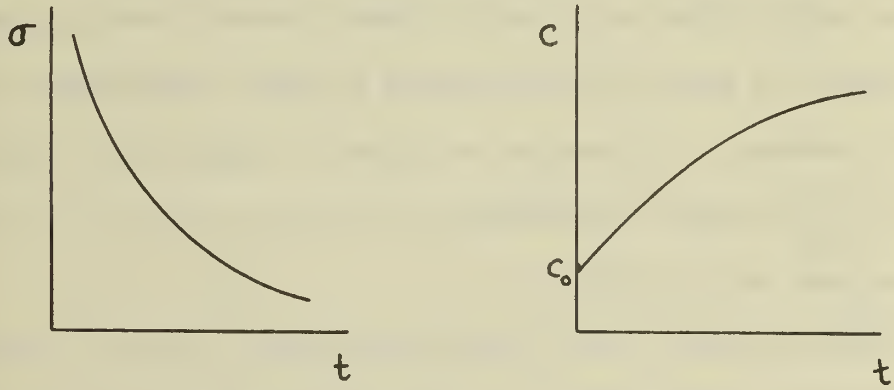

Figure 2-4 Representative Data From Strip Test

From the crack history, the crack velocity history can be constructed by taking the slopes graphically (Fig. 2-5). A cross-plot can then be made of stress, or equivalently stress intensity factor, versus crack velocity. This is the master curve, or fracture characterization curve shown in Figure 2-5. Normally these tests will be conducted over a range of temperatures in order to obtain the whole curve.

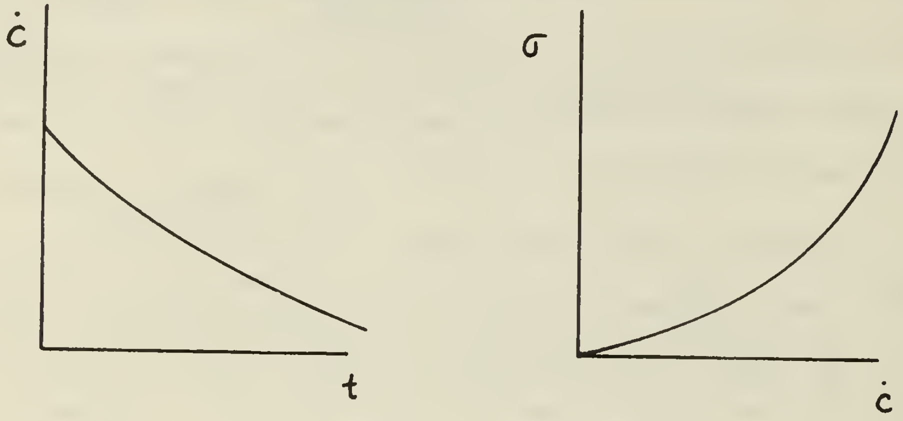

Figure 2-5

Master Fracture Characterization Curve

Hertzler[13] has obtained such characterization data over a range of temperatures from 15°F to 85°F for a CTPB propellant. He found that the data shifted very well to make a master curve, and the shift was exactly the same as that obtained by other investigators for the relaxation modulus. His results are shown in Figure 2-6. Part of the scatter in the data is attributed to the fact that the approximate expression was used to reduce it.

To our knowledge this is the first viscoelastic fracture characterization of propellant. Some scatter in the data is caused by local inhomogeneities in the material, which in turn cause the crack velocity to fluctuate as the tip proceeds through, or around, these regions. Nevertheless the master curve is well defined and exhibits no more scatter than is normally noted in propellant data of other varieties,

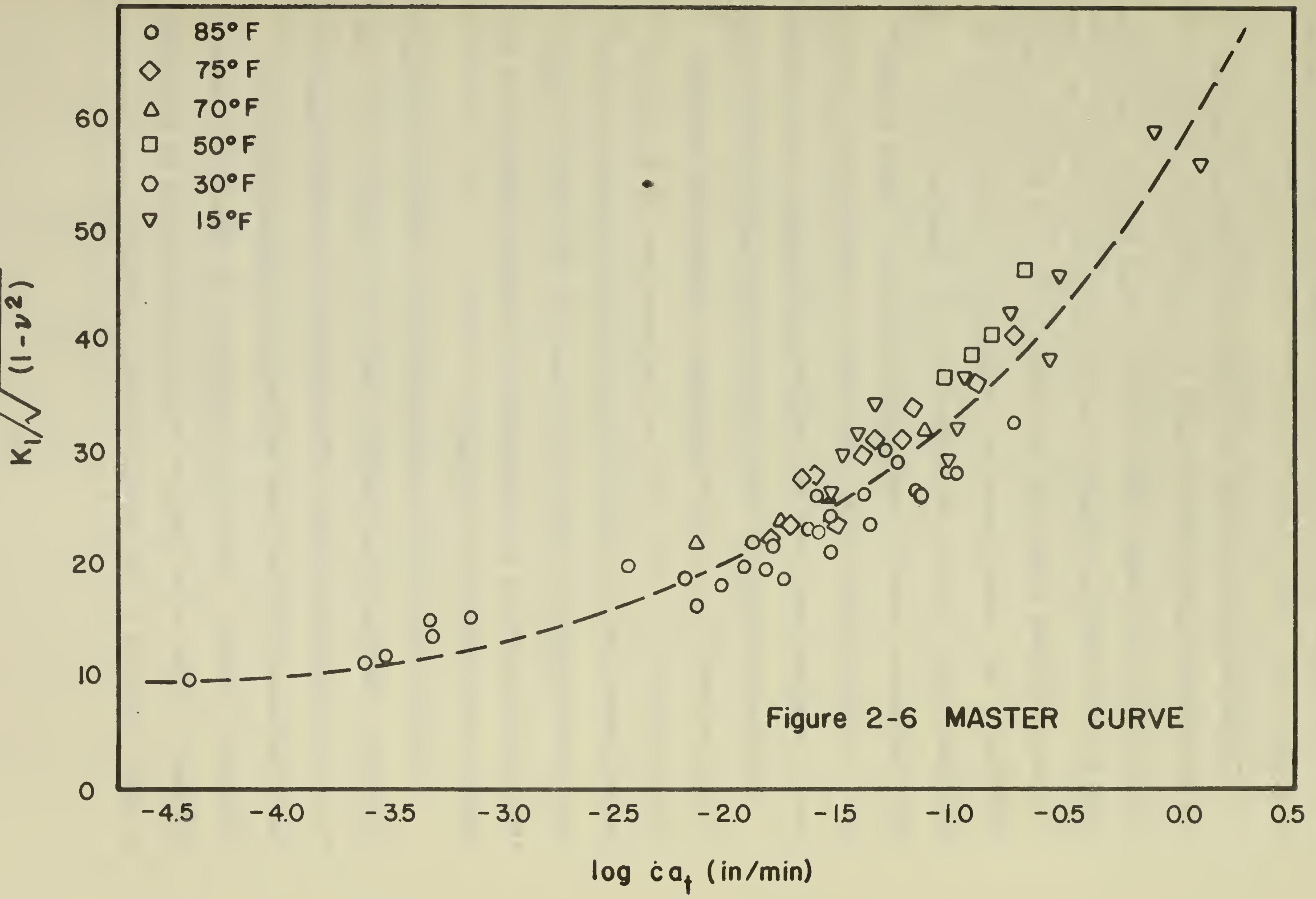

Figure 2-6 MASTER CURVE

even modulus data, which should evince the smallest amount of scatter of all.

The master curve indicates two limit values that are important. The low velocity region gives evidence of a lower bound of stress intensity factor for which there will be no crack growth. This figure of $K_{1c} = 10 \text{ psi} \sqrt{in}$ is a useful guide in making limit checks on behavior of cracks in rocket motors, from which their structural stability can be determined. Any loading below this limit should be safe, at least for the present time; however, the tendency of this characterization to change with time, as in a storage condition, is not known. Future testing could be directed toward this end; however it would require considerable amounts of propellant, since many rather large specimens are required.

Specimens selected for this characterization were marginally small in size and were 6" x 1" x 1/4" and bonded to wooden tabs along the six inch dimension. Five different specimens were run for each of the six temperatures. Of course it would be best if the entire set of tests were duplicated at each time interval of the period selected. From this information a good description of fracture behavior over the desired shelf life could be obtained.

In lieu of that data, one might assume on the basis of the results in Section 1 that the stress intensity factor will degrade in the same manner as the ultimate strength. This quantity is routinely measured in biaxial endurance data and forms the basis for extrapolating to the storage life required. With this information, the behavior of cracks existing in rocket motors that are currently stored could be predicted, and the reliability of the missile from this standpoint could be assessed.

The other end of the spectrum is also of interest. It appears that if the data were extended in the high velocity range, the ultimate limit of crack velocity would be approximately 10 inches per minute. This is indeed slow and substantiates the earlier assumptions that neglected the inertial terms in the equilibrium equations. An ultimate limit strongly influences the crack history. For instance consider an infinite sheet with a central crack subjected to a step stress at infinity. From equation (2.10)

$$K_1(t) = \sigma_o h(t)\sqrt{\pi c(t)} \tag{2.26}$$

From Figure 2-6, if $K_1(0)$ is greater than 10 psi $\sqrt{in}$, the crack will begin to grow. As it grows $K_1(t)$ increases, and in turn the crack propagates faster. This process continues until the crack reaches a limit velocity, at which time it will continue to propagate across the infinite sheet at constant speed, even though the stress intensity factor continues to increase.

The time to reach the constant velocity portion of the history is a function of the magnitude of σ_o. If σ_o were large enough, the crack could begin its propagation in the constant velocity region, in which case the behavior would be elastic, much like most observed behavior with metals or glassy polymers. On the other hand, infinite time could be required if $K(0)$ is below 10 psi $\sqrt{in}$. However any $K(0)$ above 10 psi $\sqrt{in}$ eventually will produce the constant-maximum velocity propagation for this kind of geometry, where $K_1(t)$ is continually increasing.

Solution Method

The method for predicting the crack behavior in viscoelastic materials essentially follows the method proposed by Knauss[11] for Solithane, with some variations for the relaxation behavior. For discussion purposes, consider a rocket motor with a bore crack, where it is desired to predict what the crack will do under a given loading program.

If an analytic expression for the stress intensity factor of the elastic motor geometry can be obtained, then by the correspondence principle previously discussed, the viscoelastic stress intensity factor is obtainable. Suppose it has the form

$$K_1^v(t) = \lambda[c(t)]\sigma(t)\sqrt{c(t)} \tag{2.27}$$

From the fracture characterization curve similar to Figure 2-6,

$$K_1^v(t) = f(\dot{c}) \tag{2.28}$$

Inserting equation (2.28) into (2.27), a first order differential equation in crack length is produced, which when integrated will give the desired history. Comparison of that history with storage life, or burning rates under operational conditions, will determine the detrimental effect, if any, that the crack may contribute.

Often times motor geometries are too complex to allow analytic expressions for the stress intensity factor. In this case numerical methods have been developed to find elastic stress intensity factors. Deverall and Lindsey[19] have suggested some simple methods by which these can be obtained. Subsequently numerical transforms and inversions would be necessary to obtain the final solutions. Because this is an involved solution process, an approximate method is being developed and studied, which looks very promising. It is based upon an observation by Dr. Russell Westman of UCLA that the local stress in bodies without cracks can often be related to the stress intensity factor for the same body with a crack. Progress on this development will be given in a later report.

Conclusions

It is felt that the viscoelastic crack behavior for materials in which the crack propagates slowly is predictable from the concepts developed in this section. Limitations on loading and geometry, however, must be such that symmetric crack behavior is produced. Further investigations will be made to ascertain if the concepts developed in Section 1 for mixed mode propagation can be applied to viscoelastic fracture. Further evaluations of the validity of these concepts will be made using existing data from the literature and in generating new experimental crack propagations results where needed.

SECTION 3

DEWETTING

SECTION 3

DEWETTING

Introduction

Propellant differs from classical viscoelastic materials through dewetting. Since dewetting has a pronounced influence on the stress-strain law for strain levels experienced in many rocket motors, it is necessary to investigate the influence of dewetting on fracture.

In previous reports Lindsey[15,16,17] and co-workers have developed an isotropic theory for dewettable materials. From this development a means has been formulated by which stress analyses can be carried forth while accounting for dewetting. In that theoretical treatment it has been postulated that a stress criterion for dewetting exists and that is is expressible in terms of a surface in principle stress space. Furthermore by application of Drucker's[18] Fundamental Theorem for stable materials, Wood[19] has obtained the general expression that describes the dewetting criterion for arbitrary stress states

$$J_2 + \alpha I_1^2 = \text{Constant} \tag{3.1}$$

where

$$\alpha = \frac{G^2}{9K^2} \quad \frac{dK}{dG}$$

In order to evaluate these results and the associated assumptions, experimental tests were developed and conducted for dewetting in uniaxial and triaxial stress fields.

The experiments employed a liquid dilatometer, both pressurized and unpressurized, and the pokerchip test . A brief synopsis of the experiments is presented here. At a later date the detailed treatment of the theory and experiments will be presented in LCDR J. E. Wood's PhD thesis.

Dilatometer Tests

A liquid-filled dilatometer using Dow-Corning DC-200 silicone fluid was employed for the measurement of volume change in uniaxial tensile test specimens. Load was sensed from strain gauges mounted on a flexure in line with the test specimen within the dilatometer chamber. Volume change was determined by visually measuring the fluid height in a capillary tube which permitted a minimum resolution of dilatometric strain of 0.01 per cent. In order to minimize the effect of thermally-induced variations, fluid height readings were compared with readings from a reference chamber which duplicated the test chamber in all thermal characteristics. Maximum test duration was limited to thirty minutes.

A number of different formulations of highly filled composite solid propellant were tested. However the most complete set of tests was carried out on a highly filled PBAN propellant supplied by United Technology Corporation. All of the following data were obtained on that propellant.

Constant Load Dilatometer Tests

Constant load uniaxial tension tests were conducted in the dilatometer to investigate the time-dependent nature of the onset of dewetting under small constant loads. Figure 3-1 shows dilatation vs. time for a series of five tests of the UTC PBAN. The rapid increase in dilatation observed to

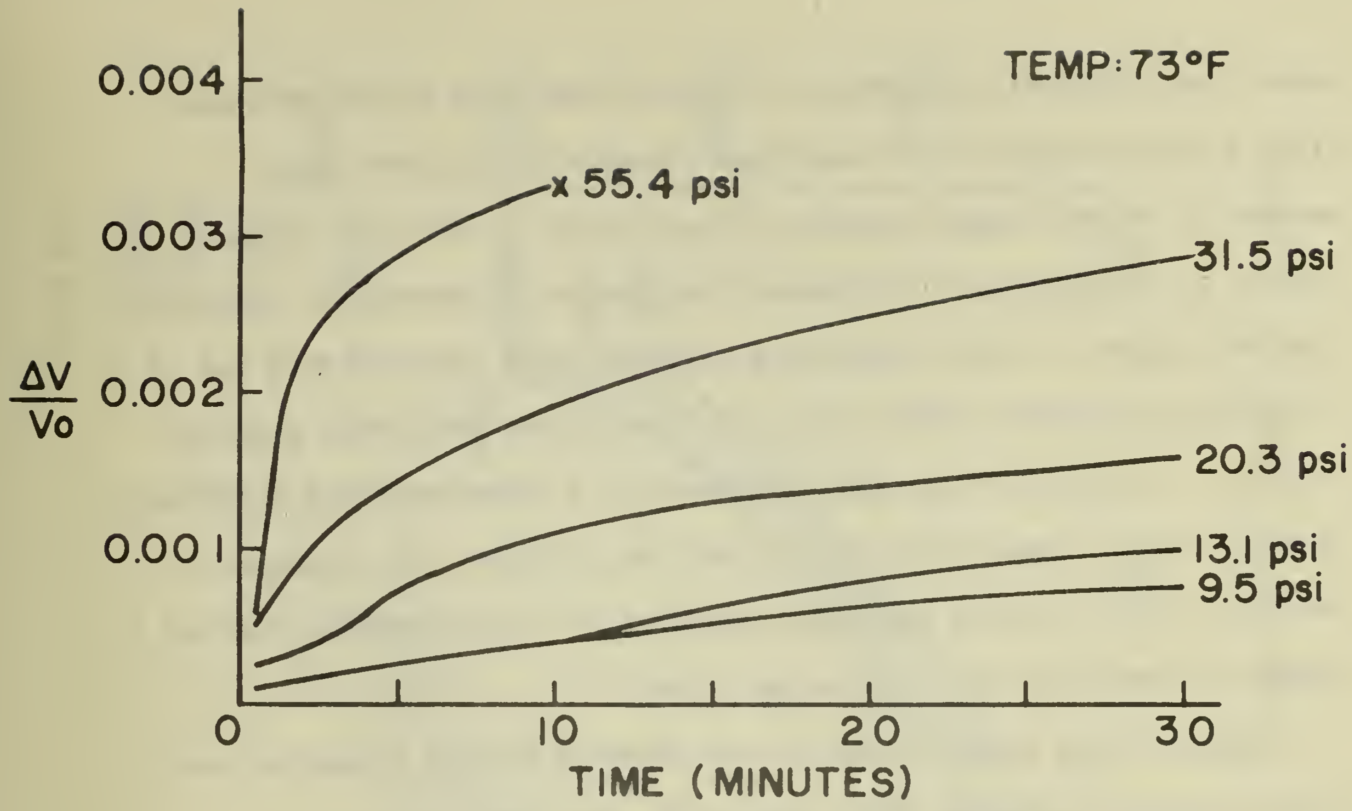

Figure 3-1

DILATATION vs. TIME AT CONSTANT LOAD, UTC PBAN

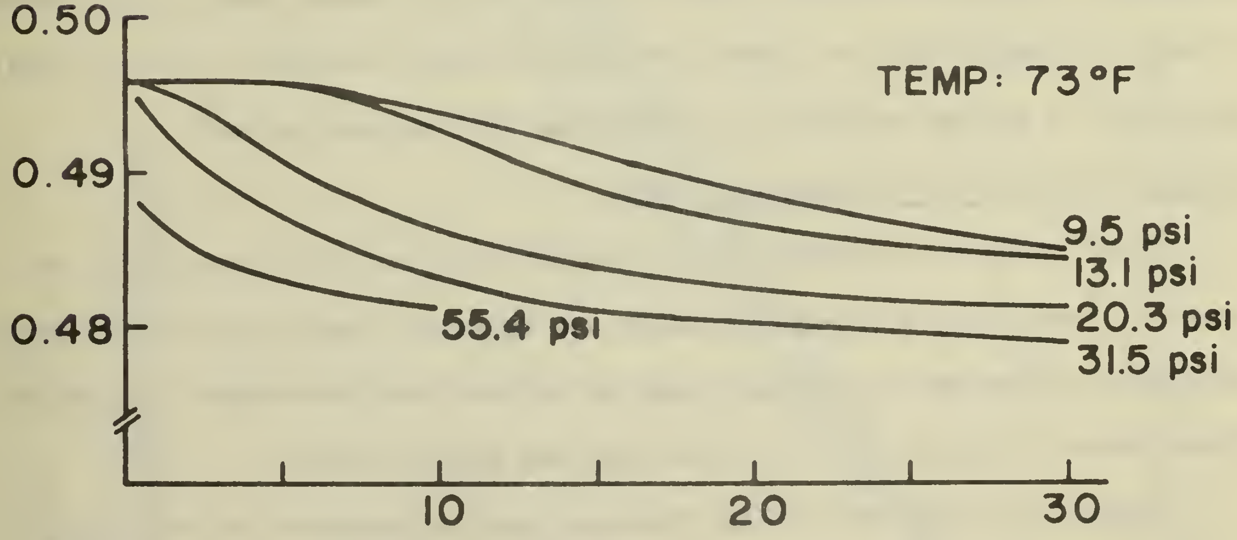

Figure 3-2

POISSON'S RATIO vs. TIME AT CONSTANT LOAD., UTC PBAN occur soon after the application of load for the three higher stresses gives a clear indication of dewetting. Because of the very small amounts of volume change produced in these tests at the lower stress levels, it is difficult to determine the presence or absence of dewetting from the figure. Further amplifying information is obtained from the variation in Poisson's ratio with time for the same specimens, shown in Fig. 3-2. In this plot the rapid decrease in ν associated with dewetting is seen to occur immediately at 55.4 psi and 31.5 psi. The response for the three lower stresses shows that the drop in ν is delayed in time and reduced in magnitude with decreasing stress.

Qualitatively similar behavior was observed for all composite propellant tested, including PBAN, PBAA, CTPB, and HTPB formulations.

From these tests, it was concluded that although the onset of dewetting in the propellants tested does demonstrate some time dependence for sufficiently small values of stress, the small amount of dilatation which results makes evaluation of this dependence impractical in the dilatometer. However, a reasonably narrow zone of stress values exists above which dewetting effects are negligible, at least for loads of short duration. It is in this sense that a stress criterion for dewetting will be interpreted.

Constant Strain Rate Dilatometer Tests.

These tests were carried out to identify the stress criterion for the onset of dewetting in uniaxial tension and uniaxial tension with superimposed hydrostatic pressure at a strain rate of one per cent per minute, for which the material response prior to dewetting was quasi-elastic.

Figure 3-3 shows the stress-strain-dilatation response for four duplicate tests of PBAN specimens. The dilatation increment plotted has the

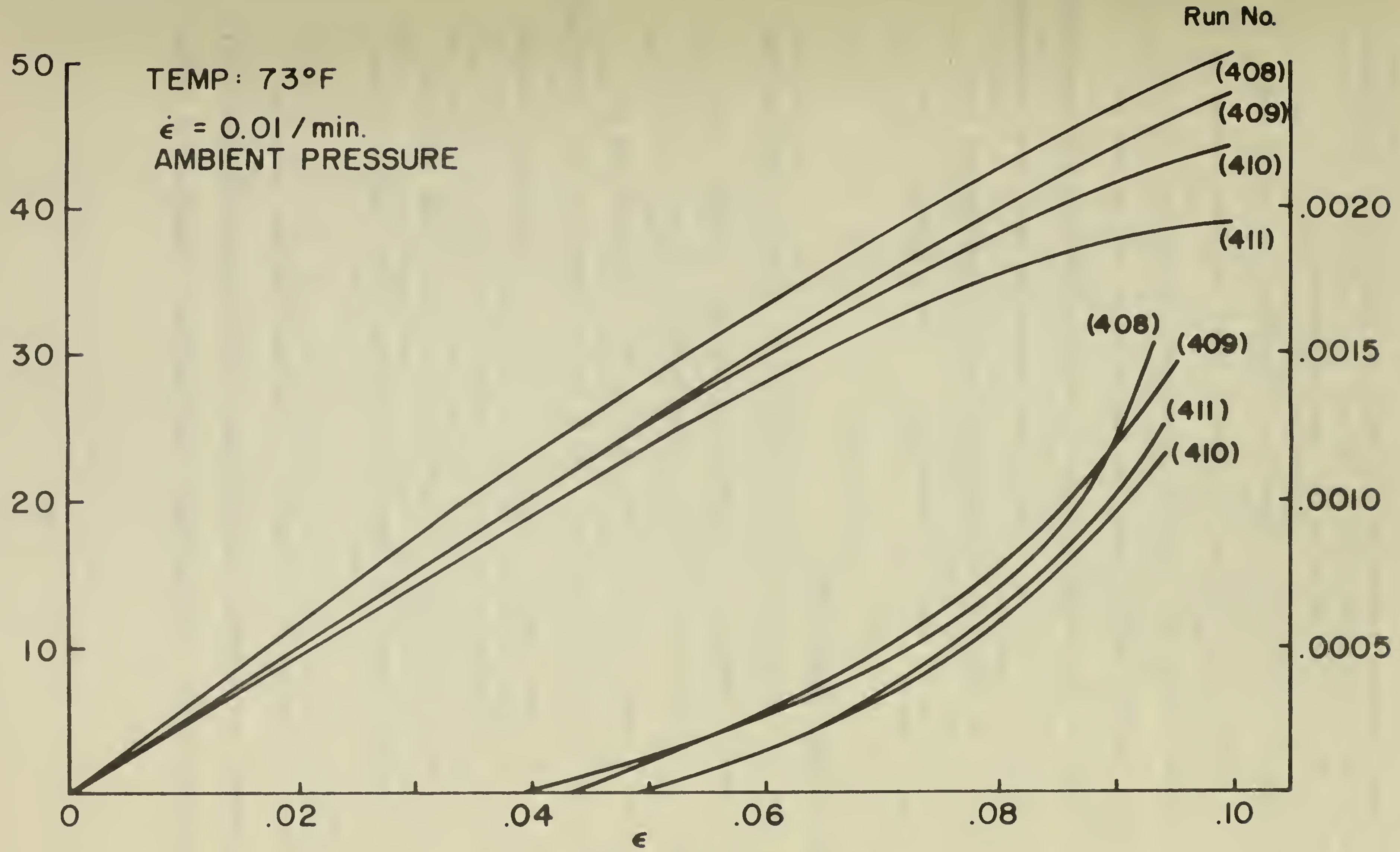

Figure 3-3
STRESS AND DILATATION vs. STRAIN-UTC PBAN CONSTANT STRAIN RATE TESTS

initial linear response subtracted out, thus the intercept of the dilatation curve with the axis indicates the onset of dewetting.

Following the above tests, pressurized dilatation tests were undertaken in an attempt to determine the onset of dewetting under a combined state of stress. Tests were run with superimposed pressures of 10, 20, and 40 psig. Maximum test pressure was limited to 40 psig because of excessive creep of the plexiglas walls of the dilatometer chamber experienced at higher pressures. More data scatter was encountered with these pressurized tests; however, no significant differences from the unpressurized tests either in the stress at onset of dewetting or in the character of the response could be detected.

Pokerchip Triaxial Tension Test

In order to investigate dewetting behavior in a stress state approximating hydrostatic tension, a pokerchip apparatus was employed. For materials with Poisson's ratio near 0.5, the pokerchip triaxial tension test provides a state of approximately hydrostatic tension within the central region of the test specimen. Using the dewetting criterion previously discussed, it is found from the analytical solution for stresses within the pokerchip that the dewetting criterion is first satisfied at the center of the specimen, within the region of hydrostatic tension. Thus the pokerchip test provides a means of initiating dewetting under a known triaxial tension state.

In order to interpret the results of the pokerchip test properly, it was necessary to determine the influence of dewetting on experimentally measurable quantities. To investigate this question a computerized finite element analysis of the pokerchip was performed. The Rohm and Haas AMG 032A structural analysis program for axisymmetric structures and loads was adapted to the IBM 360-67 computer at the Naval Postgraduate School. This program is designed to handle materials with Poisson's ratio at or near 0.5, and allows variation of material properties from element to element, thus it was suitable for the task.

To test the program and establish convergence, the program was used to analyze a pokerchip specimen loaded with a uniform axial elongation. Results were compared with the approximate analytical solution given by the LSWZ[20] analysis. The geometry chosen was that which would be used in later testing - a disk 4" in diameter and 0.25" thick. Various modulus values representative of composite solid propellant were investigated, with Poisson's ratios in the range 0.49 to 0.499. The program was found to perform satisfactorily, giving close correlation with the LSWZ solution. The program was designed to have the capability of handling incompressible material ($\nu = .5$), however, it was found that for the very stringent displacement boundary conditions imposed by the pokerchip test, convergence became less easy to achieve as ν approached 0.5. By utilizing the maximum allowable number of elements in the radial direction, it was possible to obtain good solutions for $\nu = 0.499$. Table 3-I gives a comparison of stresses calculated by the program and by the LSWZ solution for this value. The comparison is quite good, diverging slightly only near the outer radius where the LSWZ solution posseses singularities.

To model the effect of dewetting in the pokerchip test, it was considered that the initial effect of dewetting would be the alteration of material properties in a small region at the center of the specimen. For the finite element representation, a two-phase specimen was employed, having an inner core 1/2" in diameter to which reduced values of E and ν were assigned, while the properties in the rest of the pokerchip were unmodified. Figure 3-4 shows a cross-section of the finite element grid employed.

Results

It was found that most aspects of the solution for the two-phase specimen showed only slight changes as properties within the core were altered. But a significant change was noted in the state of stress around the center of the specimen, especially within the core itself, for slight variations in Poisson's ratio in the core material. Figure 3-5 shows the computed axial stress at the midplane versus radius for various values of ν at the central core. For a reduction of ν_{core} of 0.8% (from .499 to .495) the stress at the center drops by approximately 10%, with progressively greater reductions occurring as ν_{core} is further decreased. The indicated percentage change in the stress state at the center is at least an order of magnitude greater than that occurring in any of the customarily measured quantities such as total load or radial displacement on the periphery.

On the basis of this analysis it appears that a pressure transducer located at the center of one of the platens of the test rig could easily detect a deviation in the local stress state due to a small

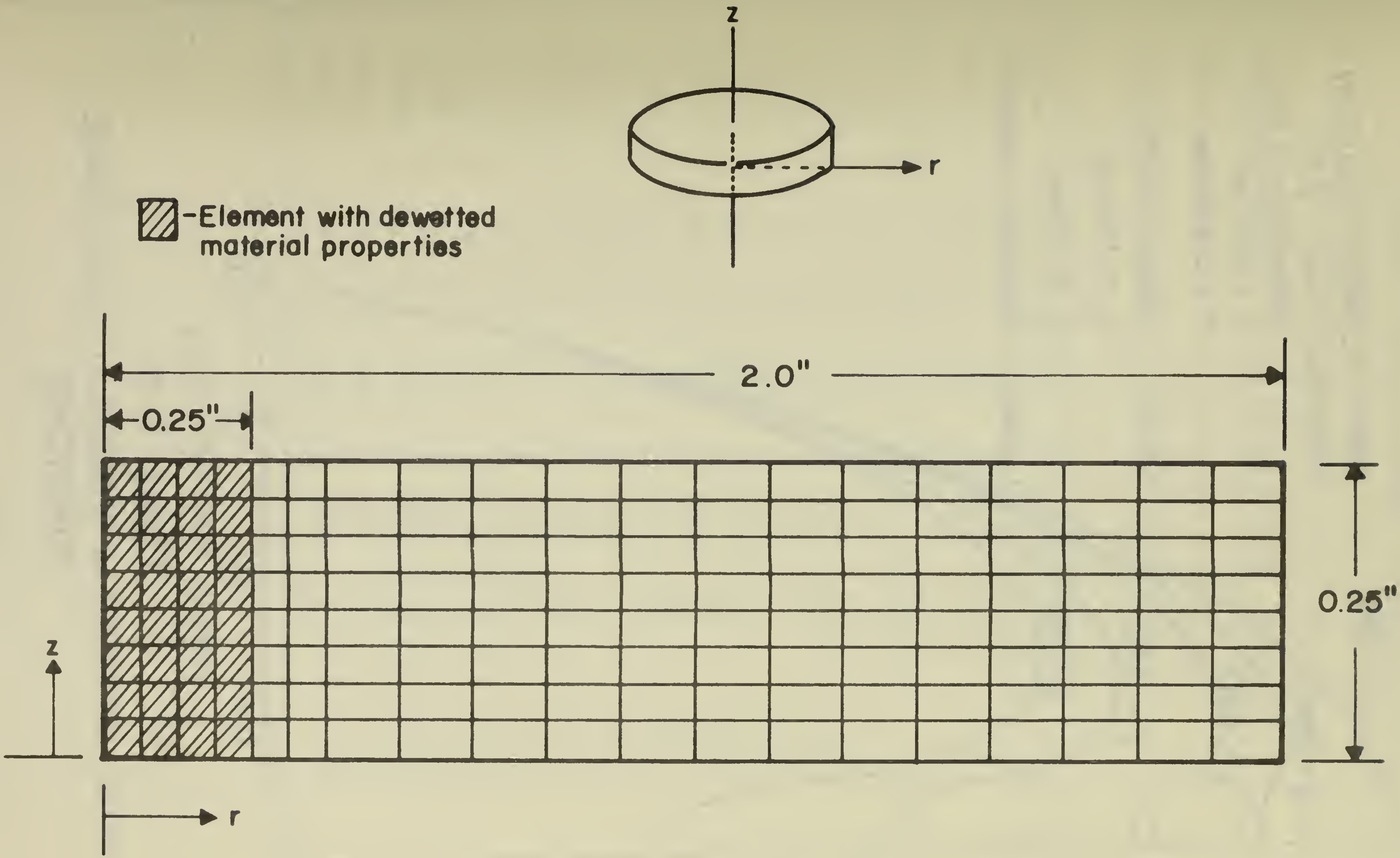
z
r
▨-Element with dewetted material properties
2.0"
0.25"
0.25"
z
r

Figure 3–4

FINITE ELEMENT REPRESENTATION OF POKERCHIP WITH DEWETTING

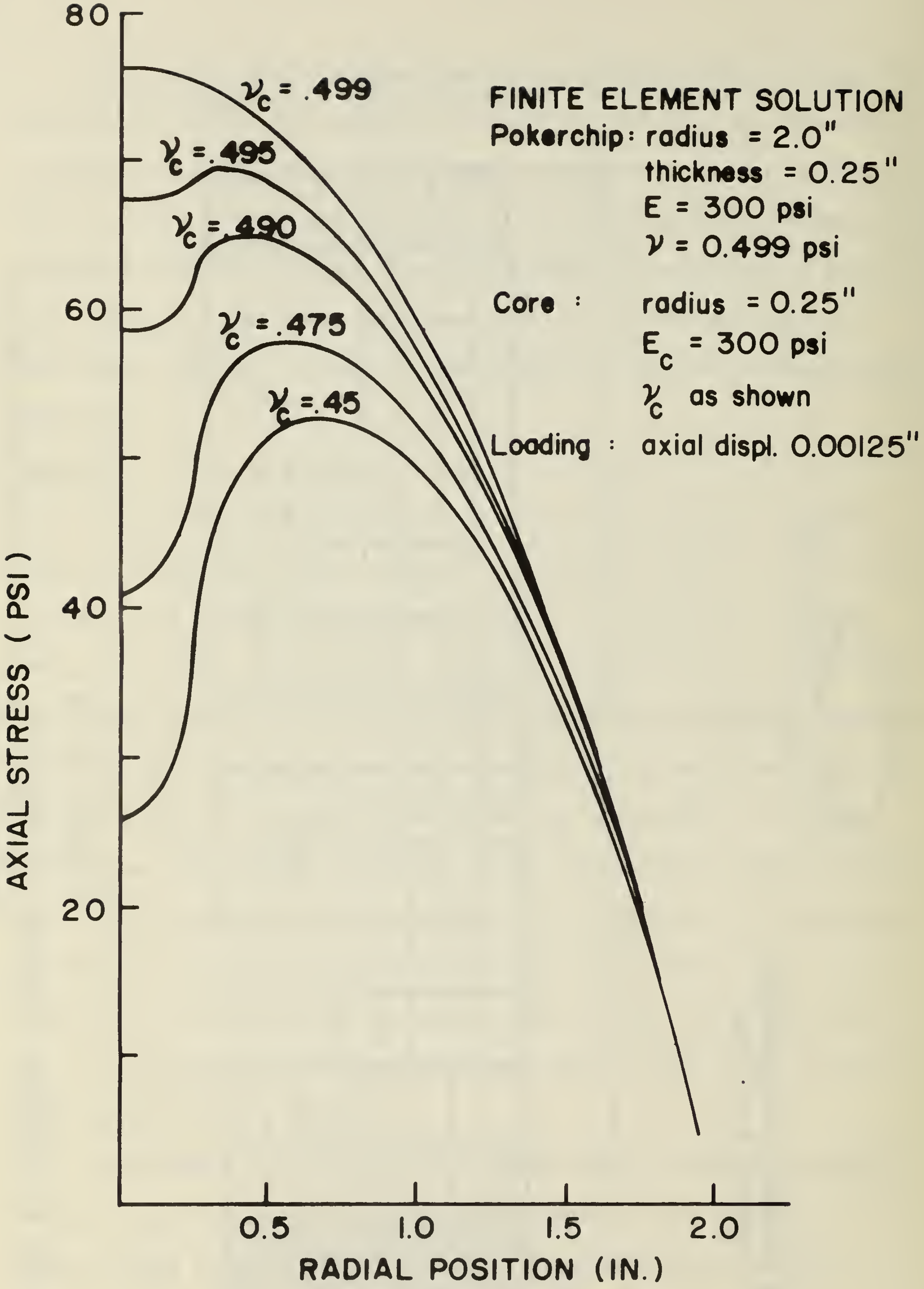

Figure 3-5

AXIAL STRESS vs. RADIUS in TWO-PHASE POKERCHIP

TABLE 3-I Midplane Stresses in Pokerchip Test Specimen

Specimen Diameter: 4.0", thickness 0.25"

Material Properties: E = 300 psi, ν = 0.499

Loading: Uniform axial elongation - $\Delta z/t$ = 0.005

Radius	Finite Element Sol.		LSWZ Sol.	Finite Element Sol.	LSWZ Sol.
Inches	σ_r PSI	σ_θ PSI	σ_r & σ_θ PSI	σ_z PSI	σ_z PSI
.0625	74.5	74.5	74.1	76.2	75.4
.1875	73.8	73.8	73.6	75.7	75.0
.3125	72.8	72.8	72.5	74.7	73.9
.4375	71.1	71.2	70.9	73.0	72.3
.5625	69.1	69.1	68.8	71.0	70.1
.6875	66.3	66.3	66.0	68.2	67.5
.8125	63.1	63.1	62.9	65.0	64.2
.9375	59.1	59.1	59.0	61.0	60.4
1.0625	54.8	54.8	54.6	56.7	56.0
1.1875	49.5	49.6	49.6	51.5	51.0
1.3125	43.9	44.0	43.9	45.9	45.3
1.4375	37.4	37.5	37.6	39.5	39.0
1.5625	30.3	30.4	30.5	32.4	32.0
1.6875	22.5	22.6	22.8	24.5	24.2
1.8125	13.7	14.2	14.3	16.6	15.8
1.9375	3.8	3.5	5.0	5.1	6.5

alteration of properties. While at present the extent to which dewetting in hydrostatic tension does alter the Poisson's ratio has not been determined, such an installation would appear to be at least as sensitive to Poisson's ratio as the dilatometer is for uniaxial testing, and should provide an equally good indication of dewetting initiation.

Another finite element problem was worked, which provided for a section of flexible boundary, just above the dewetted core, where the pressure transducer would be mounted in the otherwise rigid grip. This analysis was conducted to determine if introduction of the pressure transducer affected the stress field in the specimen. Even by allowing the displacement at the boundary to be 200 times the expected displacement of the transducer diaphragm, the change in the stress field was imperceptable.

Accordingly a pressure transducer with a 1/2" diameter contact area was imbedded in the center of one of the 4" diameter pokerchip platens, similar in construction to that reported by Harbert[21]. Figure 3-6 shows the stress-strain plot obtained from one of the pokerchip tests run at an axial strain rate of 0.007/min. The dashed lines indicate the elastic solution for the specimen with $E = 520$ psi and $\nu = .495$. At an axial strain of 0.0075, the stress sensed by the pressure transducer at the center of the specimen shows a sharp reduction from the initial linear slope. The stress level at this point, 94 psi in this case, is taken as the point of dewetting initiation.

Pokerchip tests instrumented with a central pressure transducer have been reported by Harbert. For his tests performed at a constant rate of

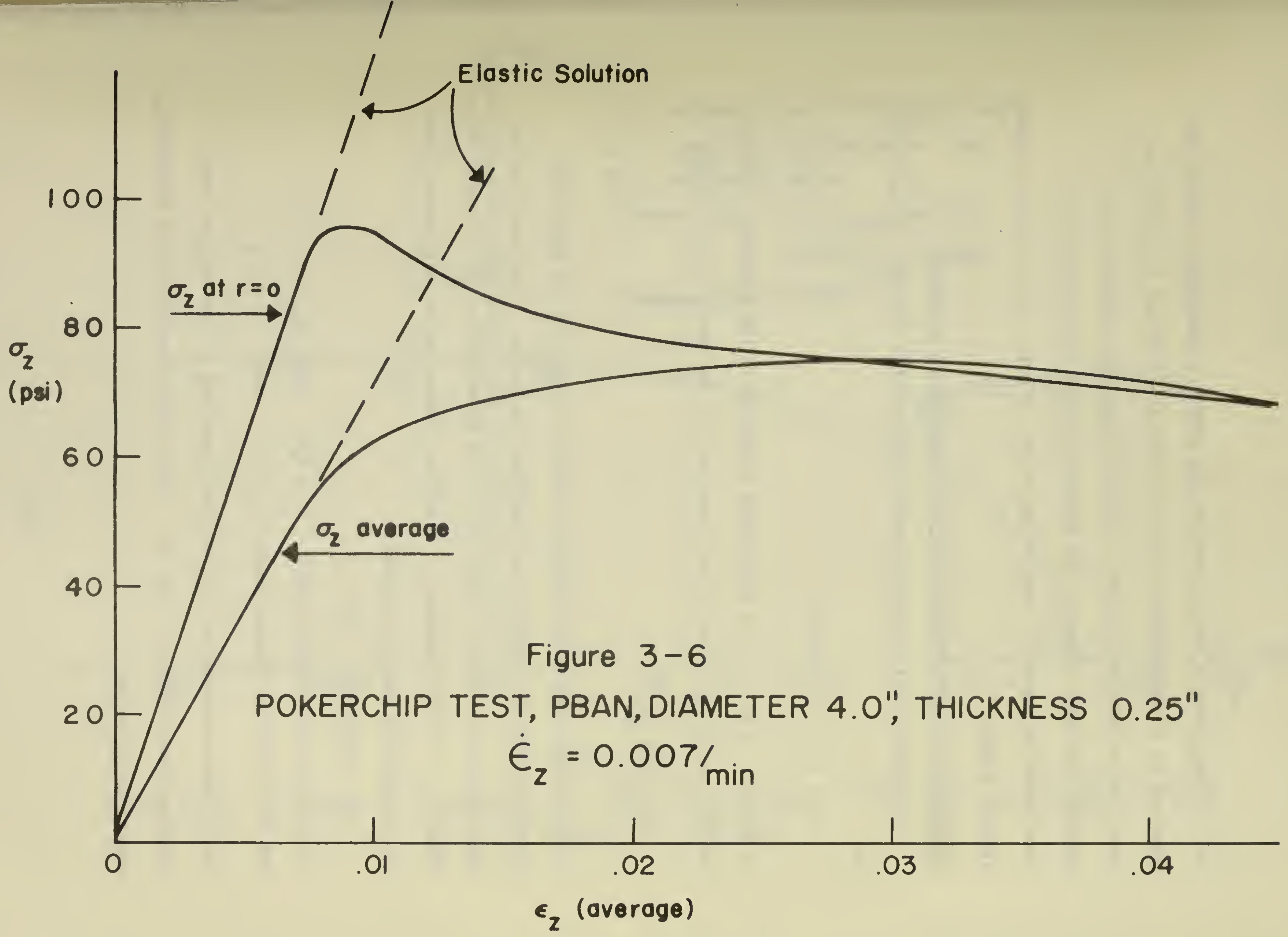

Figure 3-6

POKERCHIP TEST, PBAN, DIAMETER 4.0", THICKNESS 0.25"

$\dot{\epsilon}_z = 0.007/_{\text{min}}$

axial elongation, a sharp break in the pressure transducer reading was observed at a characteristic level of stress which was identified as the point of initial failure. From the analysis reported above, it appears that such a result may indicate only a slight reduction in load-carrying capability which may be at a stress well below the actual failure stress.

Comparison of Experimental Data with Theoretical Criterion

The theoretically derived dewetting criterion referred to previously is

$$J_2 + \alpha I_1^2 = \text{Constant} \tag{3.1}$$

in which $J_2 = \frac{1}{2}S_{ij}S_{ij}$ is the second invariant of the deviatoric stress tensor and $I_1=\sigma_{kk}$ is the first invariant of the stress tensor, while

$$\alpha = \frac{G^2}{9K^2} \frac{dK}{dG}$$

is a material parameter dependent upon the change in the shear and bulk moduli of the material as dewetting initiates. From data for the unpressurized uniaxial tensile test runs shown in Fig. 3-3 , α was calculated to be 0.0026, making the dewetting criterion for this material at the temperature and rate tested:

$$J_2 + 0.0026\, I_1^2 = 180$$

For the uniaxial tensile tests $J_2 = \sigma_u^2/3$ and $I_1 = \sigma_u - 3P$.

For the pokerchip triaxial tests $J_2 = 0$ and $I_1 = 3\sigma_t$.

The stresses measured at the point of dewetting in the various tests described are plotted in Fig. 3-7. The solid curve shows the theoretical dewetting criterion.

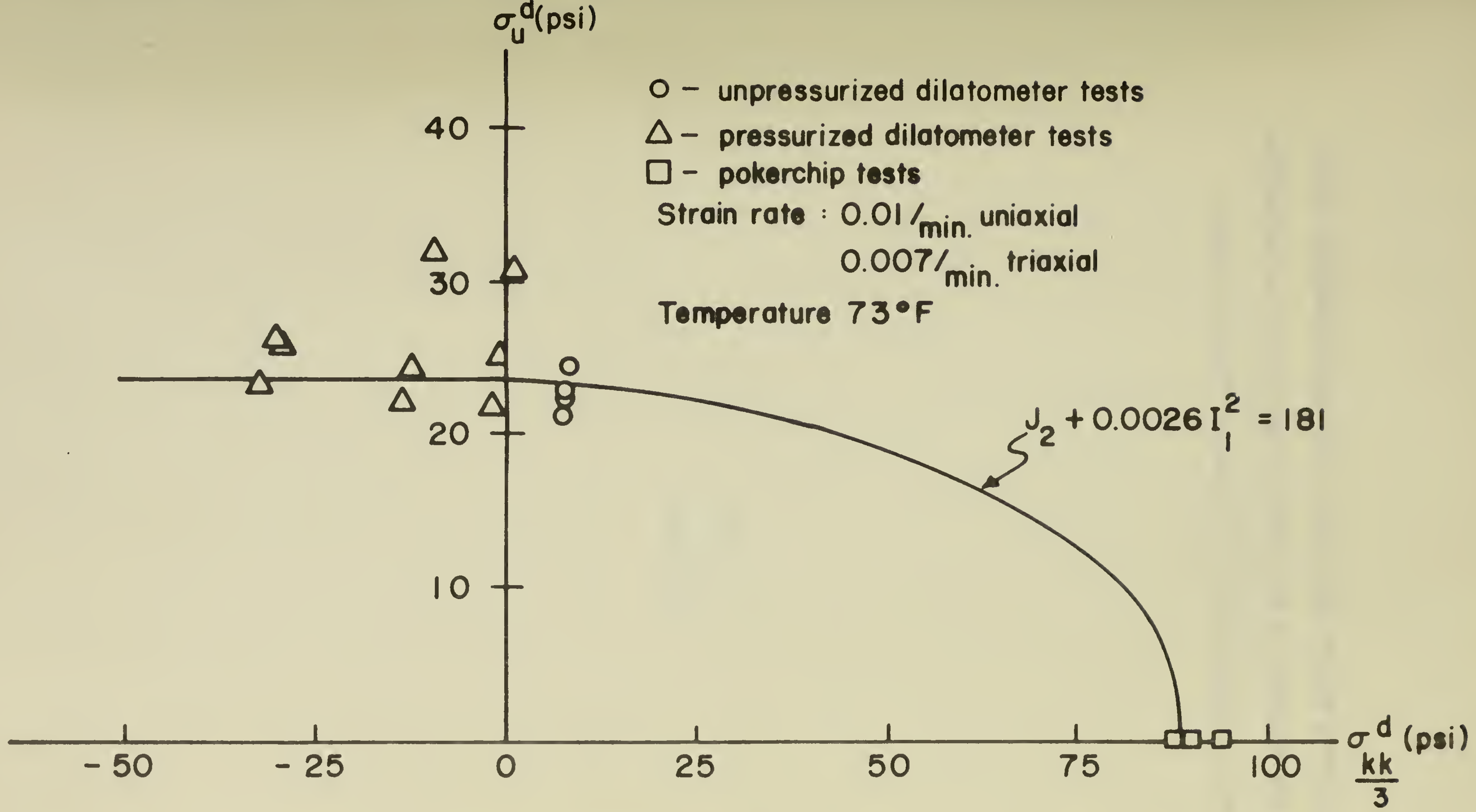

Figure 3–7

UNIAXIAL TENSILE STRESS vs. DILATATIONAL STRESS at DEWETTING INITIATION, UTC PBAN

While the limited amount and range of the data presented cannot alone confirm the validity of the stress criterion, it is satisfying to note the good correlation with the triaxial tension results.

SECTION 4

CONCLUSION

SECTION 4

CONCLUSION

Several aspects of polymer fracture have been discussed in this report. A theory for crack instability under mixed mode conditions has been proposed, and to a limited extent verified, for a glassy polymer. Normally advanced concepts such as this are first attempted on the simpler elastic materials where there exists a higher probability of success. Then once a foothold has been established, it can be generalized and made applicable to viscoelastic materials. The developments and results in Section 1 constitute work of that type and further work will be directed toward generalizing it to be applicable to viscoelastic materials and propellants.

Viscoelastic materials, being more complex, do not have so advanced a fracture theory as do elastic materials. The evolution of theory lags that of elastic materials but is following along in a very similar pattern of development. The concept of stress intensity factor for viscoelastic materials is used very extensively in this development, much more so than in the current literature on the subject. The methods proposed by which materials may be characterized for fracture and later analyzed for fracture are still hypothetical in nature and must be evaluated experimentally. This work is presently being pursued.

An alternate method of development based upon an energy approach as performed by Knauss and his coworkers, leads by a very complex analysis to a dependence in the solution on an undetermined length parameter, which must be evaluated experimentally. The approach outlined in Section 2 avoids this problem by going directly to the stress intensity factor, and it becomes much more simple mathematically.

Finally propellant fracture to be complete must incorporate dewetting effects. A theory to do this in quasielastic situations has emerged and has been experimentally evaluated for a limited number of stress states. Considerable work has been expended in developing this theory and LCDR J. E. Wood has completed a PhD research project in this area. His thesis is now in preparation and will treat this topic in detail. Copies will be forwarded when available. A brief synopsis of just a few of the results are included in Section 3 to provide an indication of the type of work that has been done.

An evaluation of what analyses can be performed at this time leads to the following conclusions:

1. Predictions of crack instability for purely elastic materials can be made for two dimensional, through the thickness cracks under arbitrary loading.
2. Predictions of crack history can be made for purely viscoelastic materials with no dewetting for two dimensional, symmetric geometries and loads.
3. Dewetting can be incorporated into the stress analysis for quasielastic loading conditions such as cool-down. Study of this problem is presently underway and the associate problem of the temperature dependence of the dewetting criterion is also being studied. Measurements of dilatation over a range of temperatures has been completed. The step to incorporate dewetting into viscoelastic materials has not yet been made.

REFERENCES

1. F. Erdogan and G. C. Sih, "On the Crack Extension in Plates Under Plane Loading and Transverse Shear." J. Basic Engineering, Dec. 1963, p. 519.

2. V. V. Panasyuk, L. T. Berezhnitskiy and S. Ye. Kovchik, "Propagation of an Arbitrarily Oriented Rectilinear Crack During Extension of a Plate," NASA Technical Translation TTF-402 from Prikladnaya Mekhanika Vol. 1, No. 2, 1965.

3. B. Cotterell, "On Brittle Fracture Paths," International Journal of Fracture Mechanics, Vol. 1, No. 2, June 1965, p. 96.

4. G. I. Barenblatt, "On Some General Concepts of the Mathematical Theory of Brittle Fracture," PMM Journal of Applied Mathematics and Mechanics, Vol. 28, No. 4, 1964, p. 778.

5. G. I. Barenblatt, "Advances in Applied Mechanics," Vol. VII, p. 55, 1962, Academic Press, New York.

6. R. L. Thorkildsen, and W. V. Olszewski, "The Effect of Biaxial Stresses on the Deformation and Fracture of Polymethylmethacrylate," Advanced Tech. Lab. Rep. 61GL181, General Electric Co., Schenectady, April 1962. Also in Engineering Design for Plastics, Edited by Eric Baer, Reinhold Publishing Corp., New York, 1964, p. 323.

7. G. C. Sih and H. Liebowitz, "Mathematical Theories of Brittle Fracture" in Fracture, An Advanced Treatise, Academic Press, 1968, p. 96.

8. H. Andersson, "Stress Intensity Factors for a Slit with an Infinitesimal Branch at one Tip," Int. Journal Fracture Mechanics, Vol. 5, No. 4, 1969, p. 371 in Reports of Current Research.

9. G.A.C.Graham, "The Correspondence Principle of Linear Viscoelasticity Theory for Mixed Boundary Value Problems Involving Time-Dependent Boundary Regions," Quarterly of Applied Mathematics, Vol 26, 1968, p 167.

10. W. G. Knauss, "Delayed Failure--The Griffith Problem for Linearly Viscoelastic Materials," International Journal of Fracture Mechanics, Vol. 6, No. 1, March 1970, p 7.

11. W. G. Knauss, "Stable and Unstable Crack Growth in Viscoelastic Media," Trans. Society of Rheology, Vol. 13, No. 3, 1969, p 291.

12. E. C. Francis, et al, "Application of Fracture Mechanics to Predicting Failures in Solid Propellants," AFRPL-TR-70-105, Air Force Rocket Propulsion Laboratory, Edwards, Calif. Sept 1970.

13. C. Hertzler, Unpublished data obtained for Engineers Degree Thesis, Aeronautics Department, Naval Postgraduate School, 1972.

14. L. Deverall and G. H. Lindsey, "A Comparison of Numerical Methods for Determining Stress Intensity Factors," to be published in the Transactions A.S.M.E. Journal of Basic Engineering.

15. G. H. Lindsey, "The Effects of Dewetting on the Fracture of Solid Propellants," NPS-57Li8121A, Naval Postgraduate School, 1968.

16. G. H. Lindsey, "The Mechanical Behavior of Dewettable Solids," NPS-57Li981A, Naval Postgraduate School, 1969.

17. G. H. Lindsey and J. E. Wood, "An Isotropic Theory for Dewettable Solids," NPS-57Li71011A Naval Postgraduate School, 1971.

18. D. C. Drucker, "A Definition of Stable Inelastic Materials," Journal of Applied Mechanics, Vol. 26, Trans. A.S.M.E.,Vol 81, Series E, 1959, p 101.

19. J. E. Wood, PhD Thesis in preparation, Aeronautics Department, Naval Postgraduate School, 1972.

20. G. H. Lindsey, et al, "The Triaxial Tension Failure of Viscoelastic Materials," ARL 63-152, Aerospace Research Laboratories, Sept 1963.

21. B. C. Harbert, "Triaxial Testing of Solid Propellants," Bulletin of 4th Meeting, ICRPG Working Group on Mechanical Behavior, Vol I, 1965, p 217.

22. W. G. Knauss and H. K. Mueller, "Crack Propagation in a Linearly Viscoelastic Strip," Journal of Applied Mechanics, June 1971, p 483.

23. W. G. Knauss and H. K. Mueller, "The Fracture Energy and Some Mechanical Properties of the Polyurethane Elastomer," Trans. Soc. Rheology, Vol 15, Issue 2, 1971, p 217.

24. W. G. Knauss and H. Dietmann, "Crack Propagation Under Variable Load Histories in Linearly Viscoelastic Solids, "Int. J. of Engineering Science, Vol 8, 1970, p. 643.

25. G. R. Irwin, "Analysis of Stresses and Strains Near the End of a Crack Traversing a Plate," J. Applied Mechanics, Sept 1957, p. 361

26. H. K. Mueller, "Stable Crack Propagation in a Viscoelastic Strip," NASA CR-1279, March 1969.

27. G. A. C. Graham, "Two Extending Crack Problems in Linear Viscoelasticity Theory," Quarterly of Applied Mathematics, Vol 27, No. 4, Jan 1970, p. 497

APPENDIX A

EXTENDED CORRESPONDENCE PRINCIPLE

The extension of the correspondence principle by Graham[9] to cover crack propagation problems is a key step in the development of viscoelastic fracture as it is done in this report. As a result, a synopsis of the central theme of the paper is included here; however the development does not parallel that of the paper but enlarges upon it. It is hoped that by reading both this appendix and the paper, a clear view of the basis for Section 2 of this report will be obtained.

Definition of the problem

The correspondence principle is clearly applicable whenever the type of boundary condition prescribed is the same at all points of the boundary. For mixed boundary value problems (i.e., problems for which different field quantities are prescribed over separate parts of the boundary) the method is still applicable provided the regions over which different types of boundary conditions are given do not vary with time. (We are, of course, assuming that the region occupied by the body does not vary with time.) There remain those viscoelastic mixed boundary value problems where the regions, over which different types of boundary conditions are given, do vary with time. Particular examples are indentation and crack propagation problems. For problems of this type there will be points of the boundary at which only partial histories of some field quantities will be prescribed. When this is the case the transforms of these quantities are not directly obtainable and the classical correspondence principle is not applicable.

We desire the solution to the viscoelastic problem shown diagramatically in Figure A-1.

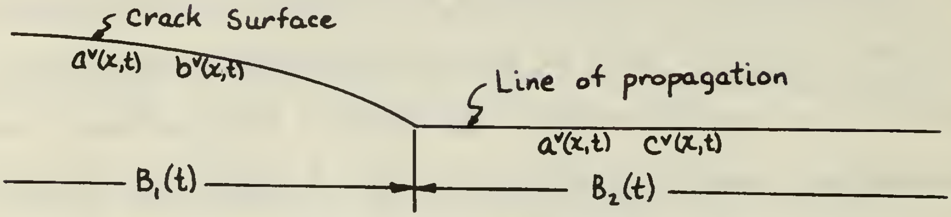

FIGURE A-1

Viscoelastic Crack Problem

In figure A-1, the material below the line of crack propagation has been removed and subsequently replaced with the appropriate boundary conditions. $a^v(x,t)$, $b^v(x,t)$ and $c^v(x,t)$ represent the elements of any column of the matrix in A.1.

$$\begin{bmatrix} \sigma_s & \sigma_s & \sigma_n & \sigma_n & u_s & u_s & u_n & u_n \\ u_n & \sigma_n & u_s & \sigma_s & \sigma_n & u_n & \sigma_s & u_s \\ \sigma_n & u_n & \sigma_s & u_s & u_n & \sigma_n & u_s & \sigma_s \end{bmatrix} \tag{A.1}$$

u_n and u_s denote normal and tangential components of the boundary displacements, and σ_n and σ_s represent similar quantities for stress. The boundary conditions for the problem are:

$$\begin{aligned} a^v(x,t) &= A^v(x,t) && \text{on} \quad B \\ b^v(x,t) &= B^v(x,t) && \text{on} \quad B_1(t) \\ c^v(x,t) &= 0 && \text{on} \quad B_2(t) \end{aligned} \tag{A.2}$$

where $B_1(t) + B_2(t) = B$, $B_1(t)$ is monotonically increasing, and B is the boundary of a fixed region R.

The solution is obtained by first solving an elastic problem with changing boundaries as shown in Figure A-2.

$\sigma^e_{ij}(x,t)$, $\epsilon^e_{ij}(x,t)$, $u^e_i(x,t)$ are solutions in R.

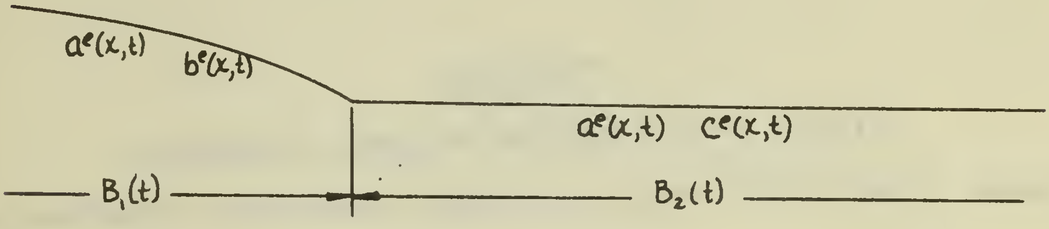

FIGURE A-2

Equivalent Elastic Problem

With the solution to this problem, the boundary values of $b^e(x,t)$ on $B_2(t)$ are computed, and the values of $c^e(x,t)$ are computed for $B_1(t)$. With these values, now define

$$\begin{aligned} b^e(x,t) &= B^e(x,t) \quad &\text{on} \quad B \\ c^e(x,t) &= k(E,\nu)\, C^e(x,t) \quad &\text{on} \quad B \end{aligned} \qquad (A.3)$$

The constraints on the problem must be such that the new boundary conditions $B^e(x,t)$ are independent of material properties. This is necessary for the classical correspondence principle to work in the next step of derivation.

We can now define the same elastic problem in terms of new boundary conditions as shown in Figure A-3

$\overset{e}{\sigma}_{ij}(x,t)$, $\overset{e}{\epsilon}_{ij}(x,t)$, $\overset{e}{u}_i(x,t)$

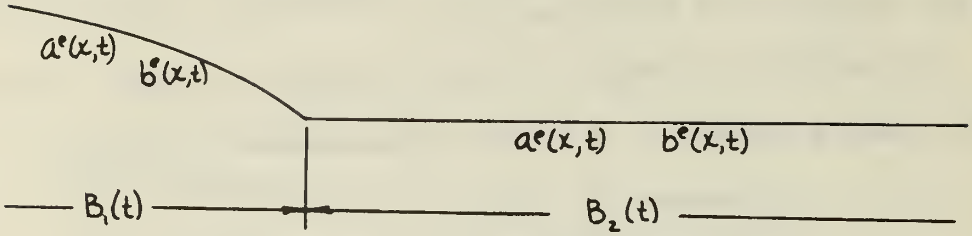

FIGURE A-3

Elastic Problem with New Boundary Conditions

Because of the nature of the new boundary conditions, transforms can be computed for them since they are now defined for all time. That condition is shown in Figure A-4.

$\overset{*}{\sigma}_{ij}$, $\overset{*}{\epsilon}_{ij}$, $\overset{*}{u}_i$ are solutions in R

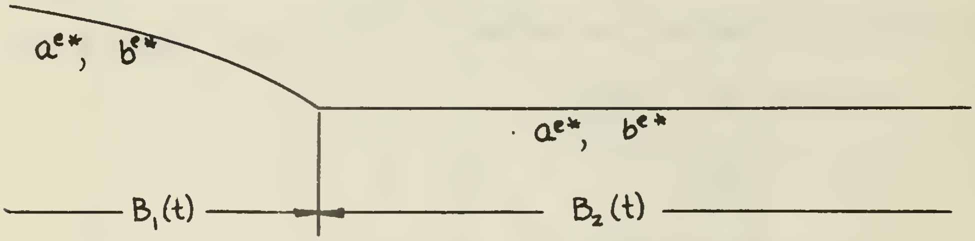

FIGURE A-4

Corresponding Elastic Problem

This is the corresponding solution for the viscoelastic problem shown in Figure A-5.

$\sigma^{v}_{ij}(x,t)$, $\epsilon^{v}_{ij}(x,t)$, $u^{v}_{i}(x,t)$ are viscoelastic solutions in R

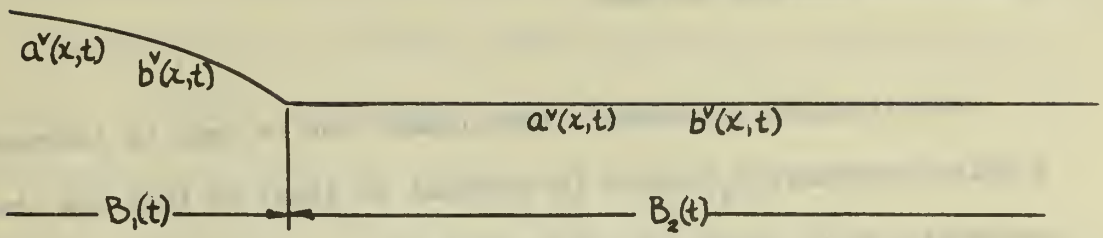

FIGURE A-5

Viscoelastic Problem Equivalent to Figure A-1

Therefore the correspondence principle is given by the classical relationships.

$$\overset{v*}{\sigma_{ij}}(x,p) = \left[\overset{e*}{\sigma_{ij}}(x,p)\right]_{\substack{E \rightarrow E* \\ \nu \rightarrow \nu*}}$$

$$\overset{v*}{\epsilon_{ij}}(x,p) = \left[\overset{e*}{\epsilon_{ij}}(x,p)\right]_{\substack{E \rightarrow E* \\ \nu \rightarrow \nu*}} \qquad (A.4)$$

$$\overset{v*}{u_{i}}(x,p) = \left[\overset{e*}{u_{i}}(x,p)\right]_{\substack{E \rightarrow E* \\ \nu \rightarrow \nu*}}$$

This extended version of the correspondence principle is used to generate theoretical developments pertaining to viscoelastic fracture.

Extension of Graham's Paper

An extension of Graham's development can be made by introducing a third boundary, B_3, which is constant in time; so that now the unchanging body region, R, is bounded by

$$B = B_1(t) + B_2(t) + B_3$$

Since B is constant,

$$B_1(t) + B_2(t) = \text{constant},$$

as in Graham's paper.

B_3 can consist of an arbitrary number of segments, upon each of which the boundary conditions may be different; however upon none of the segments can the type of boundary condition change with time.

Such a difinition of the boundary conveniently facilitates the application of the correspondence principle to finite geometries. For instance consider the infinite strip geometry with displacement boundary conditions as shown in Figure A-6.

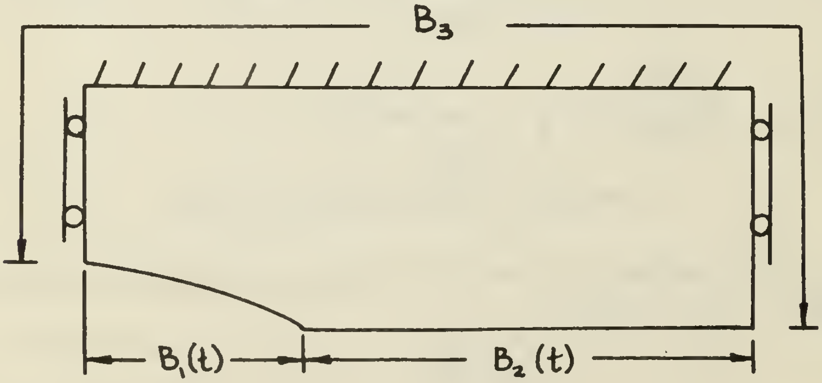

Figure A-6 Infinite Strip Subjected to Displacement Boundary Conditions

The boundary conditions on B_3 are known for all time, and therefore their transforms can be computed. Now applying the original methods of Graham, the entire development goes through as before; however now a more versatile geometry is available for which the correspondence principle is applicable. The prime limitation upon generating solutions is the requirement that $B^e(x,t)$ in equation (A.3) be independent of material properties.

APPENDIX B

STRESS ANALYSIS OF AN INFINITE STRIP

Viscoelastic crack propagation has been extensively studied by Knauss and coworkers.[10, 11, 22, 23, 24] Much of the work has been done on an infinite strip with a semi infinite crack. A simplified, but oft times adequate, solution method is given in this appendix for the stress intensity factor of the strip. The elasticity theory required is very elementary, and it is presented here for completeness in the development of the viscoelastic stress intensity factor.

Elastic Stress Analysis of Strip

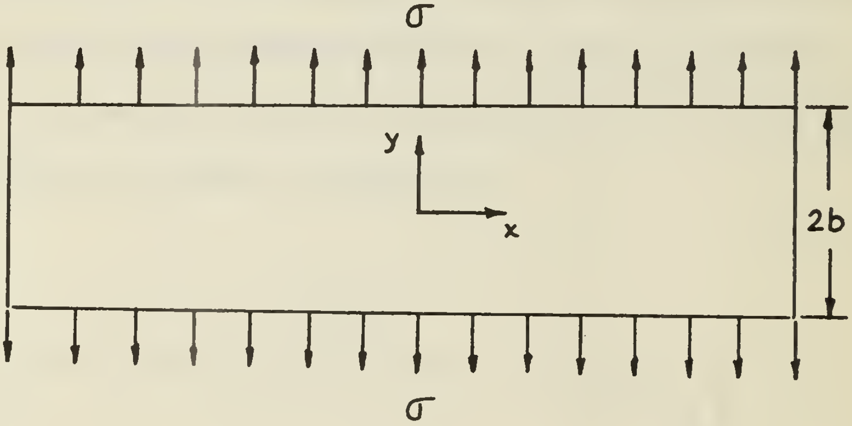

Figure B-1 Stress Boundary Conditions

The Stress Boundary Conditions are specified as

$$y = \pm b \qquad \sigma_y = \sigma \qquad \tau_{xy} = 0$$

No x = constant boundaries (infinite)

Zero stress in the x direction at infinity.

Consider a stress function of the form

$$\phi = \frac{\sigma}{2} x^2 \tag{B.1}$$

Obviously this function satisfies the biharmonic equation. The components of stress produced by this function are:

$$\sigma_x = 0 \qquad \sigma_y = \sigma \qquad \tau_{xy} = 0 \tag{B.2}$$

This stress field satisfies the boundary conditions and therefore constitutes the solution to the problem. The corresponding strain field is:

$$\epsilon_x = -\frac{\nu}{E}\sigma \qquad \epsilon_y = \frac{\sigma}{E} \qquad \epsilon_z = -\frac{\nu}{E}\sigma \tag{B.3}$$

If a semi-infinite crack is inserted in the strip, as shown in Figure B-2, the solution obtained above will be valid out in front of the crack at some distance where the disturbance caused by the crack has decayed to zero.

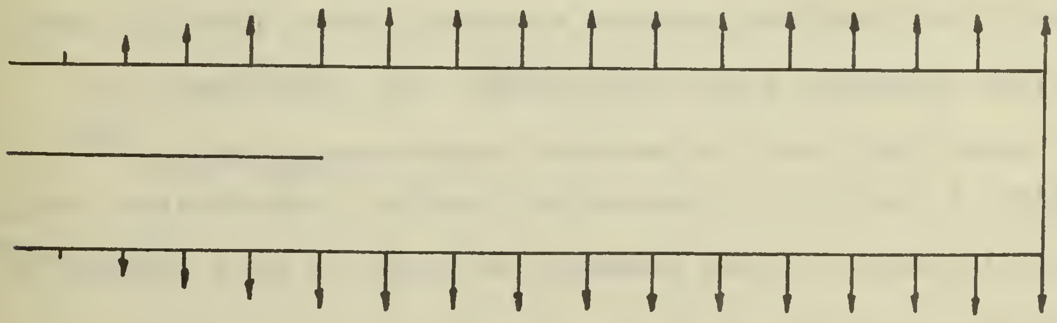

Figure B-2 Infinite Strip with a Seminfinite Crack

To the far left, the sheet is completely unloaded and stress free. To the far right it is under constant stress as if there were no crack, and in the center there is a transition region of unknown character between the two constant fields. If the crack advances by an amount Δc, the transition region moves ahead Δc. The constant stress field is reduced in dimension by Δc, and the unstressed region is increased by the same amount. The strain energy lost from the constant stress field by the crack moving ahead Δc is

$$\Delta U = \frac{1}{2} \sigma_y \epsilon_y 2bt\Delta c \tag{B.4}$$

where t is the thickness of the sheet. In the limit of infinitesimal increments in crack length,

$$\frac{dU}{dc} = \sigma_y \epsilon_y bt = \frac{\sigma^2}{E} bt \tag{B.5}$$

From Irwin's development, which related stress intensity factor and strain energy release rate for cracks in plane stress,

$$\frac{K_1^2}{E} = \frac{1}{t} \frac{dU}{dc} \tag{B.6}$$

Thus the stress intensity factor for the infinite strip is

$$K_1 = \sigma\sqrt{b} \tag{B.7}$$

It is of interest to note that this geometry is independent of crack length and therefore possesses a constant stress intensity factor as the crack propagates across the specimen. For this reason this geometry lends itself well to laboratory measurements. Mueller[26] has obtained a solution of a pressurized crack in a semi-infinite strip, and from his results, one can determine the length of crack required to produce the same effect as an infinite strip.

The difficulties encountered in experimentally holding a constant stress at the boundary as the crack moves is great enough to pursuade most investigators to use displacement boundary conditions.

Displacement Boundary Conditions

For the same strip geometry subjected to displacement boundary conditions on

$$y = \pm b \qquad u = 0 \qquad v = v_o \tag{B.8}$$

Guess a displacement field that is everywhere zero for u and is odd in y for v.

$$u(x,y) = 0 \tag{B.9a}$$

$$v(y) = a_o + a_1 y + a_3 y^3 \ldots \tag{B.9b}$$

On the centerline of the sheet, v must be zero by symmetry; therefore $a_o = 0$. The strain field corresponding to these displacements is

$$\epsilon_x = 0 \qquad \epsilon_y = a_1 + 3a_3 y^2 + \ldots \qquad \epsilon_z = \epsilon_z(x,y) \qquad \gamma_{xy} = 0 \tag{B.10}$$

The stresses that result from such boundary conditions are calculated from the stress-strain law,

$$0 = \sigma_x - \nu\sigma_y \tag{B.11a}$$

$$a_1 + 3a_3 y^2 + \ldots = \frac{1}{E}[\sigma_y - \nu\sigma_x] \tag{B.11b}$$

$$\epsilon_z = \frac{-\nu}{E}[\sigma_x + \sigma_y] \tag{B.11c}$$

From (B.11a)

$$\sigma_x = \nu\sigma_y, \tag{B.12a}$$

and

$$a_1 + 3a_3 y^2 + \ldots = \left[\frac{1-\nu^2}{E}\right]\sigma_y \tag{B.12b}$$

$$\varepsilon_z = \frac{-\nu}{E}(1 + \nu)\sigma_y \tag{B.12c}$$

The two dimensional equilibrium equations simplify to

$$\nu \frac{\partial \sigma_y}{\partial x} = 0 \qquad \frac{\partial \sigma_y}{\partial y} = 0 \tag{B.13}$$

Using equation (B.12b), equilibrium is satisfied if

$$\frac{E}{1-\nu^2}[6a_3 y + \ldots] = 0$$

Setting a_3 and all coefficients of higher order terms to zero, the solution reduces to

$$u(x,y) = 0 \tag{B.14a}$$

$$v(y) = a_1 y \tag{B.14b}$$

The boundary conditions are satisfied if $a_1 = \frac{v_o}{b}$; therefore,

$$u(x,y) = 0 \qquad v(y) = \frac{v_o}{b} y \tag{B.15}$$

The strains are obtained by differentiation.

$$\varepsilon_x = 0 \qquad \varepsilon_y = \frac{v_o}{b} \qquad \varepsilon_z = -\nu(1-\nu)\frac{v_o}{b} \qquad \gamma_{xy} = 0 \tag{B.16}$$

and the stress field is expressed by

$$\sigma_x = \left[\frac{\nu E}{1-\nu^2}\right]\frac{v_o}{b} \qquad \sigma_y = \left[\frac{E}{1-\nu^2}\right]\frac{v_o}{b} \qquad \sigma_z = 0 \qquad \tau_{xy} = 0 \tag{B.17}$$

As before, when a crack is inserted into this specimen the constant stress field of equation (B.17) is present at a distance out in front of the crack. As the crack advances, the domain of constant stress far in front of the crack is reduced by Δc, and the domain of zero stress far to the rear of the crack is increased by Δc. The energy lost in the process of the crack moving by Δc reduces to the same expression as before, even though the stress and strain fields are different.

$$\Delta U = \frac{1}{2} \sigma_y \epsilon_y 2bt \, \Delta c \qquad (B.18)$$

In the limit of infinitesimal crack increments

$$\frac{dU}{dC} = \frac{E}{1-\nu^2} \left(\frac{v_o}{b}\right)^2 bt \qquad (B.19)$$

Once again from Irwin's relationship in equation (B.6)

$$K_1 = \frac{E}{\sqrt{1-\nu^2}} \left(\frac{v_o}{b}\right) \sqrt{b} \qquad (B.20a)$$

or from (B.17)

$$K_1 = \sigma_y \sqrt{1-\nu^2} \, \sqrt{b} \qquad (B.20b)$$

DISTRIBUTION LIST

		No. Copies
1.	Arnold Adicoff Michaelson Laboratory Navy Weapons Center China Lake, California	10
2.	Defense Documentation Center Cameron Station Alexandria, Virginia 22314	20
3.	Library Naval Postgraduate School Monterey, California 93940	2
4.	Department of Aeronautics Naval Postgraduate School Monterey, California 93940	1
5.	Superintendent Naval Postgraduate School Monterey, California 93940	1
6.	G. H. Lindsey Associate Professor Department of Aeronautics Naval Postgraduate School Monterey, California 93940	5
7.	LCDR James E. Wood, USN Aero Engineering Programs Naval Postgraduate School Monterey, California 93940	1
8.	LCDR C. Hertzler Aero Engineering Programs Naval Postgraduate School Monterey, California 93940	1
9.	Eugene Francis United Technology Center 1050 East Arquez Avenue Sunnyvale, California	1

DOCUMENT CONTROL DATA - R & D

(Security classification of title, body of abstract and indexing annotation must be entered when the overall report is classified)

1. ORIGINATING ACTIVITY *(Corporate author)*
Naval Postgraduate School
Monterey, California

2a. REPORT SECURITY CLASSIFICATION
Unclassified

2b. GROUP

3. REPORT TITLE
Studies Pertaining to Solid Propellant Fracture

4. DESCRIPTIVE NOTES *(Type of report and inclusive dates)*
Technical Report

5. AUTHOR(S) *(First name, middle initial, last name)*
G. H. Lindsey

6. REPORT DATE
31 January 1972

7a. TOTAL NO. OF PAGES
71

7b. NO. OF REFS
27

8a. CONTRACT OR GRANT NO.

b. PROJECT NO.

c.

d.

9a. ORIGINATOR'S REPORT NUMBER(S)
NPS-57Li72011A

9b. OTHER REPORT NO(S) *(Any other numbers that may be assigned this report)*

10. DISTRIBUTION STATEMENT
This document has been approved for public release and sale; its distribution is unlimited.

11. SUPPLEMENTARY NOTES

12. SPONSORING MILITARY ACTIVITY

13. ABSTRACT

This study of propellant fracture has been subdivided into three parts: (1) pertinent elastic fracture developments, (2) viscoelastic fracture, and (3) dewetting.

In (1) a fracture criterion is developed for stress fields producing mixed mode crack propagation by drawing a comparison with fracture in uncracked geometries. Such mixed fields are prevalent for cracks in rocket motors with star shaped cavities.

In (2) a means for predicting crack growth and velocity has been developed for linear viscoelastic materials strictly on the basis of stress intensity factors. A fracture characterization of critical stress intensity factor for a CTPB propellant has been completed, which facilitates the application of the theory.

In (3) extensive dewetting experiments have been completed which have confirmed prior theoretical developments of a quasielastic dewetting theory. Not only has the concept of a stress criterion for dewetting been substantiated, but the form of the surface predicted by the theory has been verified.

DD FORM 1 NOV 65 1473 (PAGE 1)
S/N 0101-807-6811

A-31408

14 KEY WORDS	LINK A		LINK B		LINK C	
	ROLE	WT	ROLE	WT	ROLE	WT
Viscoelastid Fracture						
Crack Propagation						
Mixed mode fracture						
dewetting						
Solid Porpollant						
Fracture Criterion						

TL785 131892
.L73 Lindsey
Studies pertaining to
solid propellant fracture.

genTL 785.L73
Studies pertaining to solid propellant f
3 2768 001 75316 3
DUDLEY KNOX LIBRARY